

DESIGN OF DUAL POLARIZED WIDEBAND MICROSTRIP ANTENNAS

A THESIS SUBMITTED TO
THE GRADUATE SCHOOL OF NATURAL AND APPLIED SCIENCES
OF
MIDDLE EAST TECHNICAL UNIVERSITY

BY

MELTEM YILDIRIM

IN PARTIAL FULFILLMENT OF THE REQUIREMENTS
FOR
THE DEGREE OF MASTER OF SCIENCE
IN
ELECTRICAL AND ELECTRONICS ENGINEERING

JUNE 2010

Approval of the thesis:

DESIGN OF DUAL POLARIZED WIDEBAND MICROSTRIP ANTENNAS

submitted by **MELTEM YILDIRIM** in partial fulfillment of the requirements for the degree of **Master of Science in Electrical and Electronics Engineering Department, Middle East Technical University** by,

Prof. Dr. Canan Özgen
Dean, Graduate School of **Natural and Applied Sciences**

Prof. Dr. İsmet Erkmén
Head of Department, **Electrical and Electronics Engineering**

Asst. Prof. Dr. Lale Alatan
Supervisor, **Electrical and Electronics Engineering Dept., METU**

Examining Committee Members:

Prof. Dr. Nilgün Günalp
Electrical and Electronics Engineering Dept., METU

Asst. Prof. Dr. Lale Alatan
Electrical and Electronics Engineering Dept., METU

Prof. Dr. Gülbin Dural
Electrical and Electronics Engineering Dept., METU

Assoc. Prof. Dr. Özlem Aydın Çivi
Electrical and Electronics Engineering Dept., METU

M.Sc. Can Barış Top
ASELSAN A.Ş.

Date:

15 June 2010

I hereby declare that all information in this document has been obtained and presented in accordance with academic rules and ethical conduct. I also declare that, as required by these rules and conduct, I have fully cited and referenced all material and results that are not original to this work.

Name, Last name : Meltem YILDIRIM

Signature :

ABSTRACT

DESIGN OF DUAL POLARIZED WIDEBAND MICROSTRIP ANTENNAS

Yıldırım, Meltem

M. Sc., Department of Electrical and Electronics Engineering

Supervisor: Asst. Prof. Dr. Lale Alatan

June 2010, 77 pages

In this thesis, a wideband dual polarized microstrip antenna is designed, manufactured and measured. Slot coupled patch antenna structure is considered in order to achieve the wideband characteristic. Although rectangular shaped slot coupled patch antennas are widely used in most of the applications, their utilization in dual polarized antenna structures is not feasible due to space limitations regarding the positioning of two separate coupling slots for each polarization. For a rectangular slot, the parameter that affects the amount of coupling is the slot length. On the other hand when a H-shaped slot is considered, both the length of the center arm and the length of the side legs determine the coupling efficiency. This flexibility about the optimization parameters of the H-shaped slot makes it possible to position the two coupling slots within the boundaries of the patch antenna. Therefore, H-shaped slot coupled patch antennas are studied in this thesis. In order to investigate the effects of slot and antenna dimensions on the radiation characteristics of the antenna, a parametric study is performed by analyzing the antenna structure with a planar electromagnetic field simulation software (Ansoft Designer). By the help of the experience gained through this parametric study, a dual polarized patch antenna that can be used at the base

station of a cellular system (DCS: 1710–1880 MHz) is designed. Before manufacturing the antenna, dimensions of the antenna are re-tuned by considering a finite sized ground plane in the simulations. Finally, the antenna is manufactured and measured. An acceptable agreement is obtained between the measurement and the simulation results.

Keywords: Microstrip antenna, patch antenna, dual-polarized patch antenna, slot coupled patch antenna

ÖZ

ÇİFT KUTUPLU GENİŞ BANTLI MİKROŞERİT ANTEN TASARIMI

Yıldırım, Meltem

Yüksek Lisans, Elektrik ve Elektronik Mühendisliği Bölümü

Tez Yöneticisi: Yard. Doç. Dr. Lale Alatan

Haziran 2010, 77 sayfa

Bu tezde genişbantlı çift kutuplu açıklıklı mikroşerit anten tasarlanmış, üretilmiş ve ölçüm yapılmıştır. Genişbant karakteristiğini sağlamak üzere açıklıklı yapıdaki antenler değerlendirilmiştir. Dikdörtgen açıklıklı anten yapıları pek çok uygulamada kullanılmakla birlikte, çift kutuplu anten tasarımında kullanımında, her bir polarizasyon için iki ayrı dikdörtgen açıklığın konumlandırılması, yer kısıtlamaları nedeniyle pratik olarak uygun olmamaktadır. Dikdörtgen açıklıklı antende, kuplaj miktarını belirleyen parametre açıklık uzunluğudur. Bunun yanında H şeklindeki açıklıklı uygulamalarda kuplaj miktarı hem merkez hem de yan kol uzunlukları tarafından ayarlanmaktadır. Buna bağlı olarak, H şeklindeki açıklıklı anten parametrelerinin optimizasyonunun sağladığı esneklik, iki farklı açıklığın konumlandırılmasına olanak sağlamaktadır. Bu nedenle, bu tezde H şeklindeki açıklıklı antenler üzerinde çalışılmış ve optimizasyon gerçekleştirilmiştir. Açıklık ve anten boyutlarının anten ışınma örüntüsü üzerindeki etkilerinin incelenmesi amacıyla düzlemsel elektromanyetik alan simülasyon yazılımı (Ansoft Designer) kullanılarak, parametrik analizler gerçekleştirilmiştir. Parametrik analizlerden edinilen tecrübeyle, mobil haberleşme baz istasyonlarında (DCS: 1710–1880 MHz) kullanılabilecek bir çift kutuplu yama anten tasarımı yapılmıştır. Anten üretiminden önce sonlu

boyuttaki toprak düzlem göz önünde bulundurularak, anten boyutları yeniden düzenlenmiştir. Sonuçlara uygun olarak anten üretimi yapılmış ve ölçümler alınmıştır. Ölçüm ve simülasyon sonuçları arasında kabul edilebilir bir uygunluk gözlenmiştir.

Anahtar kelimeler: Mikroşerit anten, yama anten, çift kutuplu yama anten, açıklıklı yama anten.

To My Dear Family
and
Serdar, my endless love...

ACKNOWLEDGEMENTS

I would like to express my gratitude to my supervisor Asst. Prof. Dr. Lale Alatan for her supervision, advice, criticism, encouragement and insight throughout the research. I would like to thank Prof Dr. Nilgün Günalp, Prof Dr. Gülbin Dural, Assoc. Prof. Dr. Özlem Aydın Çivi and Can Barış Top for serving in my committee and sharing their opinions.

I also would like to thank ASELSAN A.Ş. for the facilities provided during my graduate degree, production of the antennas and TÜBİTAK-BİDEB (The Scientific and Technological Research Council of Turkey-The Department of Science Fellowships and Grant Programmes) for its support to scientific research.

I would like to express my special and deepest thanks to my love, Serdar, for giving me the strength and courage to complete this thesis. He has been an excellent supportive during all part of the studies and measurements. Without his support, I would not be able to accomplish this work.

Lastly, I would like to express my endless gratitude to my dear family for trusting in me regardless of any circumstance.

TABLE OF CONTENTS

| | |
|-------------------------------------------------------------------------------------------------------|------------|
| ABSTRACT | IV |
| ÖZ | VI |
| ACKNOWLEDGEMENTS | IX |
| TABLE OF CONTENTS | X |
| LIST OF TABLES | XI |
| LIST OF FIGURES | XII |
| CHAPTERS | |
| 1. INTRODUCTION | 1 |
| 2. ANALYSIS OF APERTURE COUPLED MICROSTRIP PATCH ANTENNAS | 9 |
| 2.1 Analysis Methods for Microstrip Patch Antennas | 9 |
| 2.2 Parameters of Aperture Coupled Patch Antennas | 16 |
| 3. DESIGN OF APERTURE COUPLED PATCH ANTENNAS | 19 |
| 3.1 Parametric Analysis of Rectangular Aperture Coupled Microstrip Patch Antenna ... | 19 |
| 3.2 Parametric Analysis of H-Shaped Slot Coupled Microstrip Patch Antenna | 36 |
| 3.3 Parametric Analysis of Dual Polarized H-Shaped Slot Coupled Microstrip Patch Antenna | 54 |
| 4. FABRICATION AND MEASUREMENTS | 58 |
| 4.1 Results of the Antenna | 63 |
| 5. CONCLUSIONS AND FUTURE WORK | 71 |
| REFERENCES | 73 |

LIST OF TABLES

TABLES

| | |
|--------------------------------------------------------------------------------------------------|----|
| Table 1-1 Application of Microstrip Antennas..... | 1 |
| Table 3-1 Design parameters of rectangular slot coupled microstrip patch antenna at 2.21GHz..... | 21 |
| Table 3-2 Design parameters of H-shaped slot coupled microstrip patch antenna at 2.21GHz..... | 37 |
| Table 3-3 Optimized parameters of dual H-shaped slot coupled microstrip patch..... | 57 |

LIST OF FIGURES

FIGURES

| | |
|--------------------------------------------------------------------------------------------------------------------------------------------------------------------|----|
| Figure 1-1 Different feed types for microstrip antennas, a) coaxial probe feed, b) microstrip line feed, c) proximity coupled feed, d) aperture coupled feed [13]. | 4 |
| Figure 1-2 Various types of coupling apertures: | 6 |
| Figure 2-1 Geometry of a rectangular microstrip patch antenna. | 10 |
| Figure 2-2 Patch enlargements as a result of fringing fields. | 11 |
| Figure 2-3 Equivalent magnetic currents for a) TM_{10} mode and b) TM_{01} mode. | 13 |
| Figure 2-4 Original problem for the aperture coupled antenna. | 14 |
| Figure 2-5 Equivalent problem for the aperture coupled antenna. | 15 |
| Figure 2-6 Aperture Coupling Feed [5]. | 16 |
| Figure 3-1 Substrate parameters. | 20 |
| Figure 3-2 Antenna structure with corresponding design parameters. | 20 |
| Figure 3-3 Input impedance as a function of stub length. | 22 |
| Figure 3-4 S_{11} as a function of stub length. | 22 |
| Figure 3-5 Input impedance at a single frequency for different values of the stub length ($f=2.21\text{MHz}$). | 23 |
| Figure 3-6 Antenna input impedance as a function of slot length. | 24 |
| Figure 3-7 Calculated input impedance as a function of aperture length. | 25 |
| Figure 3-8 View of the antenna structure for different values of x_{of} . | 26 |
| Figure 3-9 Effect of x_{of} on input impedance loci. | 27 |
| Figure 3-10 Effect of x_{of} on input return loss. | 28 |
| Figure 3-11 View of the antenna structure for different values of y_{of} . | 29 |
| Figure 3-12 Effect of y_{of} on input impedance. | 30 |
| Figure 3-13 Effect of y_{of} on input return loss. | 31 |
| Figure 3-14 Effect of the permittivity of the antenna substrate for different ϵ_a values a) $\epsilon_a=2.54$, b) $\epsilon_a=3.38$. | 32 |
| Figure 3-15 Return loss graph for different values of ϵ_a a) $\epsilon_a=2.54$, b) $\epsilon_a=3.38$. | 33 |

| | |
|------------------------------------------------------------------------------------------------------------------------------------------------------------------------------------------------------------------|----|
| Figure 3-16 Return loss graph for different values of the thickness of the feed substrate; a) $d_a=1.6\text{mm}$, b) $d_a=3.2\text{mm}$, c) $d_a=4.8\text{mm}$ | 34 |
| Figure 3-17 Return loss graph for different values of the thickness of the feed substrate; a) $d_a=1.6\text{mm}$, b) $d_a=3.2\text{mm}$, c) $d_a=4.8\text{mm}$. (Continued) | 35 |
| Figure 3-18 Microstrip fed “H-shaped slot coupled patch antenna” parameters..... | 36 |
| Figure 3-19 Input impedance as a function of stub length..... | 38 |
| Figure 3-20 S11 as a function of stub length LM from 4mm to 20mm..... | 39 |
| Figure 3-21 Input impedance at a single frequency for different values of the stub length ($f=2.21\text{MHz}$). | 40 |
| Figure 3-22 Input impedance as a function of l_{s1} | 41 |
| Figure 3-23 Return loss as a function of l_{s1} | 42 |
| Figure 3-24 Input impedance as a function of ws_2 | 43 |
| Figure 3-25 Return loss as a function of ws_2 | 44 |
| Figure 3-26 Effect of xof on input impedance..... | 45 |
| Figure 3-27 Effect of xof on input return loss. | 46 |
| Figure 3-28 Effect of the patch position to input impedance..... | 47 |
| Figure 3-29 Effect of the patch position to input impedance..... | 48 |
| Figure 3-30 Sizes of the rectangular slot and H-shaped slot at 2.21GHz. | 49 |
| Figure 3-31 Return loss graphs of a) rectangular slot, b) H-shaped slot coupled patch antennas..... | 50 |
| Figure 3-32 Radiation characteristics of rectangular slot coupled patch antenna ... | 51 |
| Figure 3-33 Radiation characteristics of H-shaped slot coupled patch antenna a) E-plane, b) H-plane..... | 53 |
| Figure 3-34 Side view of dual H-shaped slot coupled patch antenna structure..... | 54 |
| Figure 3-35 Top view of dual H-shaped slot coupled patch antenna structure | 55 |
| Figure 3-36 Return loss graph for S11 and S22 with an infinite ground plane. | 56 |
| Figure 4-1 Return loss graph for S11 and S22 with a finite ground plane. | 59 |
| Figure 4-2 Initial fabrication process of the patch and feed layers, a) antenna patch structure, b) antenna ground plane with the H-shaped slots, c) microstrip lines feeding the patch from H-shaped slots..... | 60 |

| | |
|------------------------------------------------------------------------------------------------------------------------------------------------------------------------------------------------------------------------------------------------------------------------------|----|
| Figure 4-3 Fabrication process after the foam is attached between feed layer and antenna layer and connectors are mounted to the microstrip lines, a) patch on top of the foam structure, b) back view of the antenna and microstrip lines, c) top view of the antenna. | 61 |
| Figure 4-4 Antenna Radiation Pattern Measurement Set-Up, a) antenna in the anechoic chamber, b) radiation pattern measurement from port 1, so port 2 is matched with a 50ohm load. | 62 |
| Figure 4-5 Experimental and simulation results for S11 (return loss)..... | 63 |
| Figure 4-6 Experimental results and Simulation results for S22 (return loss)..... | 64 |
| Figure 4-7 Experimental and simulation results for S12 (Isolation between port 1 and port 2). | 65 |
| Figure 4-8 Radiation pattern characteristics port 1 excitation for a) simulation b) measurement results respectively, E-plane..... | 66 |
| Figure 4-9 Radiation pattern characteristics port 1 excitation for | 67 |
| Figure 4-10 Radiation pattern characteristics port 2 excitation for a) simulation b) measurement results respectively, E-plane..... | 68 |
| Figure 4-11 Radiation pattern characteristics port 2 excitation for a) simulation b) measurement results respectively, H- plane, | 69 |
| Figure 5-1 Electric field lines and effective dielectric constant geometry of microstrip patch antenna [5]. | 76 |

CHAPTER 1

INTRODUCTION

“The microstrip antenna is composed of a patch structure, a dielectric substrate and a ground plane [4]”. The basis of the radiation in microstrip patch antenna is discontinuities and bends of the printed patch. “Patch is positioned on one part of the dielectric substrate and the ground plane is on the other part [4]”. There are various alternative patch shapes for microstrip antennas such as rectangular, circular, square and ring type patches. The most commonly used version is the rectangular patch antenna due to its advantageous radiation characteristics and ease of fabrication. Microstrip antennas were first introduced by Deschamps in 1953 [1].

However, the first practical implementations were performed by Howell and Munson in the early 1970's [2] [3]. Since then, microstrip antennas are widely used in various commercial systems, whose examples are listed in Table 1-1, because of the numerous advantages they offer.

Table 1-1 Application of Microstrip Antennas.

| Application | Frequency |
|----------------------------|---------------------------|
| Paging | 931-932 MHz |
| GSM | 900 MHz and 1800 MHz |
| Global Positioning System | 1575 MHz and 1227 MHz |
| Direct Broadcast Satellite | 11.7-12.5 GHz |
| Collision Avoidance Radar | 60 GHz, 77 GHz and 94 GHz |
| Automatic Toll Collection | 905 MHz and 5-6 GHz |

It is mentioned that, “the most important advantage of the microstrip antenna is the size” [4], which provides easier installation to systems like mobile communication infrastructures. They are also low profile and lightweight structures. Secondly, the fabrication of the microstrip antennas is easier and reliable. Microstrip antennas are produced with printed circuit board processes, which are fast and cost effective. Besides, the microstrip antennas are reliable, in terms of reproducibility “such that the new copies of the antenna follow the characteristics of the first produced unit” [4]. More than the advantages in fabrication, construction of antennas with all the necessary circuits on the same substrate makes them compact. It is even possible to produce the boards with connecting drills and to add active and passive elements to the antenna. It is worth to mention the disadvantages of the microstrip antennas, for the awareness of the preventive measures to be considered within the antenna design.

First of all, the output power level of the microstrip antennas is low compared with other types of antennas [5] [6]. The physical characteristics of these antennas could not handle high power levels. Besides, the efficiency levels are also low. The next important “disadvantage of the microstrip patch antenna is the narrow bandwidth” [5] . In general, the frequency bandwidth of the microstrip antennas is at most few percents [5] [6].

In parallel with the technology breakdown in mobile and satellite communications, and biomedical applications, the need for low cost, low volume, lightweight antennas has been extensively increased. Since most of these practical needs are satisfied by microstrip antennas, extensive research has been conducted to overcome the problems associated with the disadvantages of these beneficial antenna structures. Critical studies have been conducted especially for the improvement of the narrow bandwidth since it forms the major obstacle for the application in the communication systems.

To enhance the value of bandwidth characteristics of the microstrip antennas can be performed by two methods.. While the first method achieves a wideband operation by utilizing a second resonant structure with a resonance frequency is near to operating frequency of patch antenna, the second group concentrates on novel feeding techniques “that would make it possible to excite the microstrip patch located on a dielectric substrate of high thickness and small dielectric constant” [7]. The later approach is preferred in this study. Therefore, first the former method will be summarized to clarify why it was not a proper choice within the scope of this thesis and then the second method will be explained in more detail.

The additional resonant structure utilized in the first approach is generally a second patch parasitically coupled to the radiating patch antenna [7]. Since the parasitic patch requires another dielectric substrate, this method results in a multilayer microstrip antenna structure. However, the fabrication of multilayer printed structures is slower, more expensive and prone to manufacturing errors due to alignment problems. Therefore, stacked patch configurations are not preferred in commercial applications. Another approach to obtain closely spaced two resonances is to reactively load the patch antenna. “The reactive loading can be achieved by cutting a U-shaped slot [8] or a notch [9] on the radiating patch”. This type of modification disturbs the current distribution on the radiating patch and increases the cross-polarization levels. Since the design of dual polarized antennas is aimed in this work, these types of structures are not preferred due to the degradation in polarization characteristics.

Before going into the details of the method implemented in this study “to broaden the bandwidth of the antenna” [8], it is worth mentioning the feeding techniques used to excite microstrip antennas. Most commonly used feed types are “coaxial probe feed, microstrip line feed, proximity coupled feed and aperture coupled feed” [13] (see Figure 1-1). First two feeding methods (a) and (b) are preferred in most of the applications due to ease of production and availability of analytical methods or equivalent circuit models that makes the analysis of the antenna computationally

efficient. The major drawback about these feed structures is the constraint on dielectric substrate. “Microstrip antenna printed on a thick dielectric substrate with low dielectric constant provides larger bandwidth”[10], because of the increase in the fringing fields. However, in coaxial probe feed structure a thick substrate corresponds to a long inner conductor that gives rise to inductive input impedance for the antenna. To eliminate “the inductive part of the input impedance”, capacitive elements could be included to feed behind the patch [10] within the connector structure or “on the surface of the patch”[11]. Hence, the manufacturing process becomes troublesome. Besides, in microstrip line feed structure, a thick dielectric substrate with low dielectric constant causes spurious feed radiation that degrades the antenna performance [5]. The dielectric substrate of the microstrip line should be thin with high dielectric constant in order to confine the guided waves directly under the line. These conflicting requirements about the choice of dielectric substrate could only be satisfied by utilizing dielectric substrates with different dielectric constants for the radiating part and the feed part as in proximity coupled and aperture coupled feed structures [12].

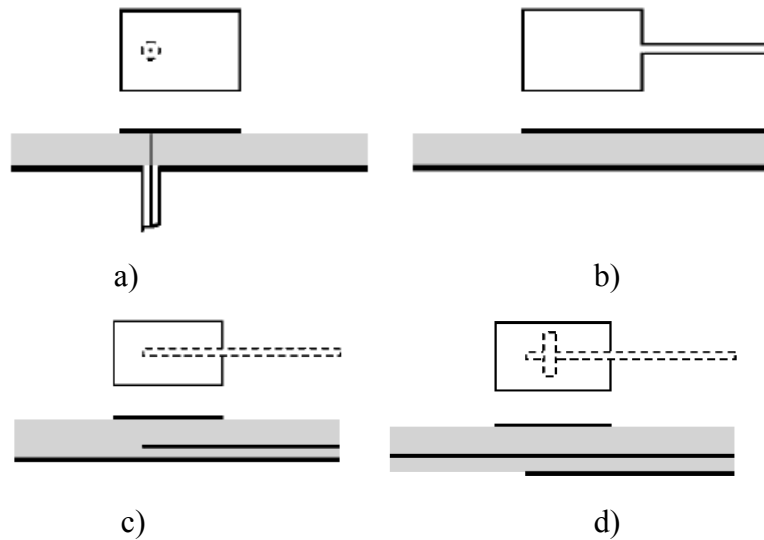


Figure 1-1 Different feed types for microstrip antennas, a) coaxial probe feed, b) microstrip line feed, c) proximity coupled feed, d) aperture coupled feed [13].

Matching of the antenna and feed structure for proximity coupled feeding method is obtained adjusting feed line location, compared with the patch. Since there is only one optimization parameter, sometimes a considerable match could not be achieved for thick dielectric substrates. On the other hand, aperture coupled feed structures offer large number of optimization parameters such as aperture shape and dimensions, offset values of the feed line compared with the center of the aperture. Also, ground plane in the aperture coupled feed structure, provides isolation between the feed line and patch, which prevents virtual radiation effect of feed on antenna radiation pattern and polarization purity [14]. It is also worth to mention that, aperture coupled feed structure provides larger space for dielectric substrate and this characteristic of the aperture coupled feed structure makes it appropriate for assembling antennas in array construction. [11]. Hence aperture coupled feed structures are studied in this thesis.

“The first introduction of the aperture coupled microstrip patch antenna performed from a graduate student, Allen Buck, in 1984 with a circular aperture” [15]. After the introduction of aperture coupled microstrip antenna, different slot shapes have been considered by researchers. Coupling amount is mostly affected from slot parameters of aperture coupled antennas. Different shapes of coupling slots satisfy to optimize antenna radiation and coupling characteristics with slot parameters. “Thin rectangular coupling slots commonly used for aperture coupled microstrip antennas. Slots with enlarged ends, such as dogbone, bow-tie, or H-shaped apertures (Figure 1-2) further improve coupling and results in a larger impedance bandwidth [16].”

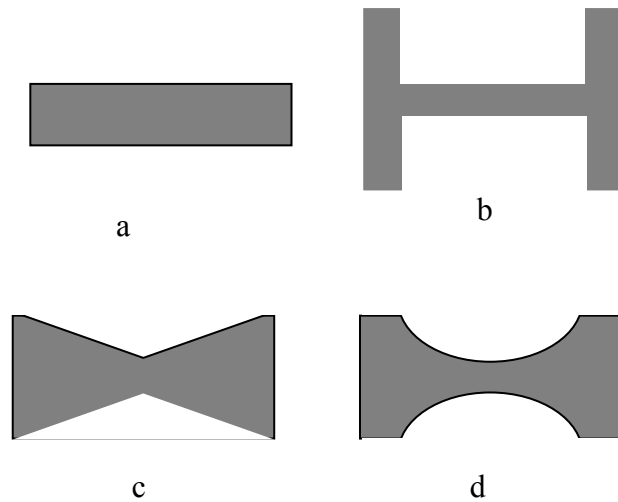


Figure 1-2 Various types of coupling apertures:
 a) Rectangular, b) H-shaped, c) Bow-tie, d) Dogbone.

In addition to the amount of coupling, the amount of radiation from the aperture shall be considered to decrease the level of antenna back radiation. Therefore, it is required to use an aperture shape, which provides maximum coupling with the smallest area [17]. H-shaped aperture fulfills this requirement. “Shin and Kim came up with a wideband and high-gain microstrip antenna coupled with H-shaped aperture [18]. Within their proposal, they achieved %24 bandwidth with a gain of 10.4 dBi at 2.05 GHz.”

The purpose of this thesis is designing a microstrip patch antenna that can be used at the cellular system base station and operating in 1710–1880 MHz frequency band. In order to achieve this bandwidth with microstrip antennas bandwidth enhancement techniques need to be applied. “This communication system also requires a dual polarized antenna in order to maximize the received signal, reduce the effects of multipath fading and enhance the channel throughput by increasing the transmission capacity per frequency [19].” In a microstrip antenna, dual polarization operation is obtained by simultaneously exciting the two orthogonal

modes of the radiating patch. Therefore two separate coupling apertures are required. For a rectangular aperture, parameter that affects the amount of coupling is the slot length. On the other hand when an H-shaped aperture is considered, both the length of center arm and side legs determine coupling efficiency. “Consequently H-shaped slot provides more design flexibility compared with the rectangular shaped slot and makes it possible to position the two coupling slots within the boundaries of the patch antenna. [16]” Gao designed “a wideband (%21), dual polarized microstrip patch antenna by using H-shaped slots [16]”. This approach satisfied “cross-polarization levels better than 22 dB for both principle planes” [16]. Considering the advantages fitting with the aim of this thesis, it is decided to design the antenna with H-shaped aperture.

In Chapter 2, the analysis methods for aperture coupled patch antennas are presented. The design parameters for rectangular and H-shaped aperture coupled antennas are also defined.

In Chapter 3, parametric analysis has been conducted for rectangular and H-shaped aperture coupled microstrip antennas through the use of electromagnetic simulation software Ansoft Designer®. The analyses of the critical parameters for two alternative structures (rectangular and H-shaped apertures) are provided with the simulation results. Chapter 3 also discusses the advantages and drawbacks of each alternative following the analysis. Based on the simulation results, the same bandwidth and return loss characteristics are obtainable with small sized H-slot architecture compared with a conventional rectangular slot at 2.21 GHz. In the light of the experience gained through the parametric analysis, a dual polarized patch antenna operating at 1710–1880 MHz frequency band is designed by optimizing the critical parameters.

Following this optimization of design parameters, “a microstrip patch antenna prototype with two H-shaped slots” is fabricated and measured. Chapter 4 covers the fabricated antenna design with information regarding the production process

and provides the evaluation of the measurement results. Comparison and evaluation of the deviations from the designed and fabricated antennas are also discussed in Chapter 4.

Finally, conclusions of this thesis work including the future work suggestions are provided in Chapter 5.

CHAPTER 2

ANALYSIS OF APERTURE COUPLED MICROSTRIP PATCH ANTENNAS

2.1 Analysis Methods for Microstrip Patch Antennas

Different methods exist to analyze microstrip antennas. “Transmission line model and cavity model are simple and useful models that provide physical insight about the radiation mechanism of the antenna.[5]” However, these are approximate models and their accuracy are less compared to full-wave analysis methods that are based on the numerical solution of integral and/or differential equations associated with the structure.

Transmission line model is useful in design process for estimating initial parameters of the antenna. The relation of the antenna length with the resonance frequency will be summarized here. The geometry of a probe fed rectangular microstrip antenna is as in Figure 2-1.

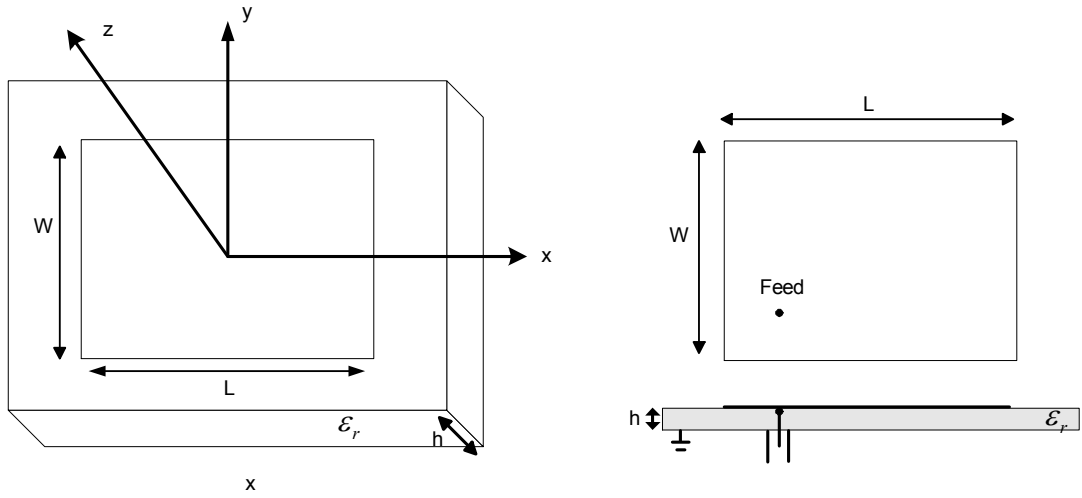


Figure 2-1 Geometry of a rectangular microstrip patch antenna.

The dimensions of the patch are not infinite and this leads fringing fields on the edges as in Figure 2-2. “The dielectric constant and height of the dielectric substrate affect the amount of fringing”[20]. Physical dimensions of microstrip patch seem greater than its actual dimensions “due to fringing effect”[20]. “The fringing fields at the two open ends are accounted for by adding equivalent lengths ΔL at both ends. The expression for ΔL is given as”[20].

$$\Delta L = 0.412h \frac{(\epsilon_e + 0.3) \cdot \left(\frac{W}{h} + 0.264 \right)}{(\epsilon_e - 0.258) \cdot \left(\frac{W}{h} + 0.8 \right)} \quad (2.1)$$

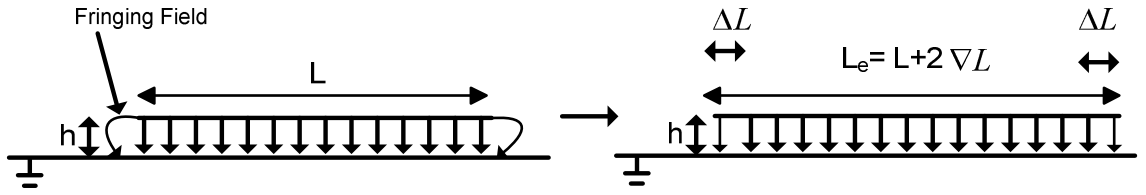


Figure 2-2 Patch enlargements as a result of fringing fields.

Patch enlargements occur for each side, so effective length of patch due to fringing fields become

$$L_e = L + 2 \Delta L \quad (2.2)$$

For a rectangular patch, first resonant occurs when the effective length L_e , shown in Figure 2-2 is half of guided wavelength (λ_d) to be calculated as

$$\lambda_d = \frac{\lambda_0}{\sqrt{\epsilon_e}} \quad \text{where} \quad \lambda_0 = \frac{c}{f} \quad (2.3)$$

ϵ_e is “the effective dielectric constant for the radiating part of the antenna”. ϵ_e calculation for microstrip line is presented in the Appendix. ϵ_e of patch can be calculated by using same formulas and by “replacing the width of the line with the width of the patch” [20].

Finally, resonance frequency of the patch is expressed by patch length as

$$f_r = \frac{c}{\lambda_d \sqrt{\epsilon_e}} = \frac{c}{(2(L+2\Delta L))\sqrt{\epsilon_e}} \quad (2.4)$$

and c is “the speed of the light”.

“In transmission line model, the patch antenna is represented in terms of an equivalent circuit. In this circuit, the patch is modeled by a transmission line of length L . The characteristic impedance and propagation constant of the line can be calculated by using the formulas presented in the Appendix.[24]” As it will be explained in the cavity model section, radiation occurs from the edges at $x=0$ and L . Therefore, these edges are modeled by an admittance that represents the radiation losses and by a capacitance that accounts for the stored energy due to the fringing fields. The transmission line model is originally proposed for probe fed microstrip antennas where equivalent circuit models are available. In parallel with the developments about new feed structures, equivalent circuit models for them are also studied in literature. The equivalent circuit model for rectangular aperture coupled microstrip antennas are defined in [21]. Once patch and feeding structures are represented by equivalent circuits, “the variation of the input impedance of the antenna with the frequency can be analyzed” [21]. Although this model is useful for predicting impedance characteristics of antenna, it does not provide any information about the radiation properties of the antenna.

Cavity model is useful in understanding the radiation mechanism of microstrip antennas. “In cavity model, microstrip antenna is treated as a cavity bounded by perfect magnetic walls on the edges and perfect electric conductors on the top and bottom surfaces.[24]” Since the dielectric substrate is generally thin, it is assumed that the field has no z dependence. Then the suitable field solutions within the cavity are:

$$E_z = C_{nm} \cos \frac{n\pi x}{L} \cos \frac{m\pi y}{W} \quad (2.5)$$

and C_{nm} is amplitude of corresponding TM_{nm} mode. The first two dominant modes will be TM_{01} and TM_{10} . By using E_z , equivalent magnetic currents can be found “around the periphery of the patch” as in Figure 2-3. It can be observed that,

radiations from edges at $y=0$ and $y=W$ cancel each other (non-radiating edges) the radiations “from the edges at $x=0$ and $x=L$ ” add up (radiating edges) for TM_{10} mode. Also the feed should be located along the $y=W/2$ line in order to excite only the TM_{10} mode. In that case the antenna will be linearly polarized in x-direction. Similar observations can be made for the TM_{01} mode. Therefore, to decrease the cross-polarization levels for a dual polarized antenna, two feed locations should be chosen along the two lines bisecting the patch in each direction.

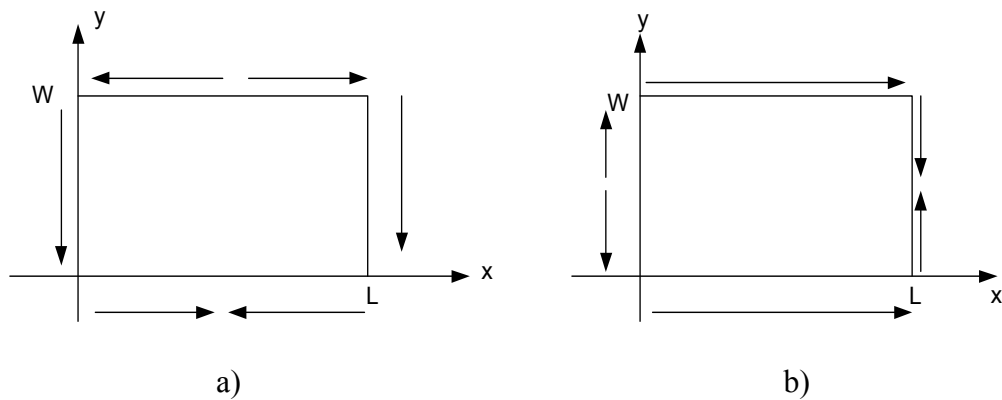


Figure 2-3 Equivalent magnetic currents for a) TM_{10} mode and b) TM_{01} mode

“Although transmission line model and cavity model provide physical insight about the radiation mechanism of the antenna, full-wave analysis techniques should be preferred in the analysis of complex structures for the sake of the accuracy” [21]. The most commonly used numerical method in the full-wave analysis is Method of Moments (MoM). In this method, “the tangential electric field components are written in terms of the surface electric currents at the surface of the patch through the use of the Green’s functions for the grounded dielectric substrate” [21]. By equating the tangential field components on the patch to zero “an integral equation

is obtained in terms of the surface currents”. Then “unknown surface currents” are expanded as known basis functions and the differential equation is transformed into a matrix equation by the use of testing functions. The solution of this matrix equation gives “the amplitudes of the basis functions”. After finding the current distribution on patch, it is possible to calculate the “input impedance and radiation pattern of the antenna” [21]. In the MoM analysis, the equivalent magnetic currents on aperture are expanded also, as of basis functions and “the continuity of the tangential component of the magnetic field is enforced at the aperture to find the amplitudes of these additional basis functions”. The MoM solution of aperture coupled microstrip antennas is presented in [22]. The electromagnetic simulation software Ansoft Designer, used in this thesis, is also based on this full-wave analysis method. Therefore, the key points of the MoM solution procedure will be summarized here.

In Figure 2-4 and Figure 2-5, a schematic of the antenna and the feedline structure and the equivalent problem defined for the MoM solution are presented, respectively.

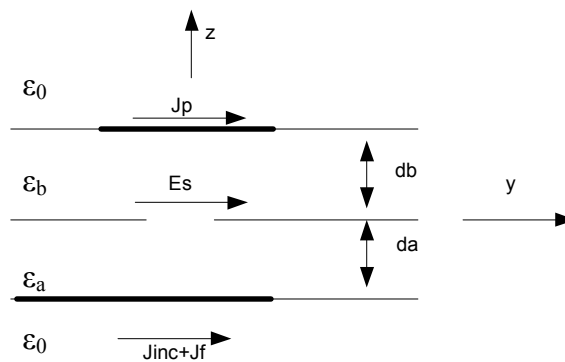


Figure 2-4 Original problem for the aperture coupled antenna.

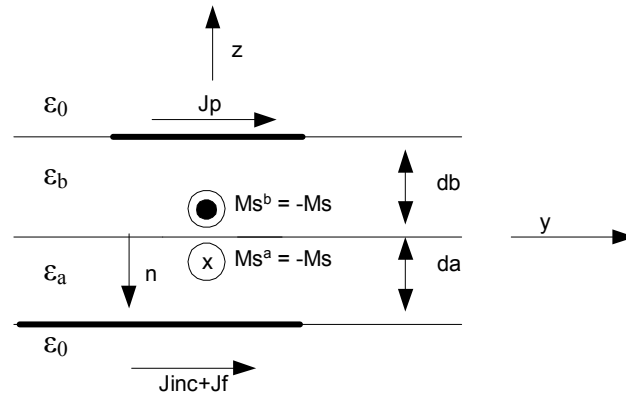


Figure 2-5 Equivalent problem for the aperture coupled antenna.

“The electric surface currents on the feedline are assumed to be y-directed. By using the equivalence principle, the aperture can be closed off with the ground plane” [21]. To keep the field distribution the same, magnetic surface currents on both sides of the aperture are assumed to be x-directed. The x-directed current density is assumed as uniform for feedline and y-directed current densities are assumed to be uniform for the aperture. Boundary conditions can be written as;

- The tangential (y-directed) electric field is zero along the microstrip line.
- The tangential magnetic field is continuous across the aperture.
- The tangential (x-directed and y-directed) electric field is zero along the patch.

“Three coupled integral equations are obtained for three unknown currents J_f, M_s, J_p and solved by applying MoM procedure”[22].

In the next section the parameters of aperture coupled patch antennas will be defined.

2.2 Parameters of Aperture Coupled Patch Antennas

Figure 2-6 represents “the geometry of the aperture coupled patch antenna”. “The radiating microstrip patch element is printed on the top of the antenna substrate, and the microstrip feed line is printed on the bottom of the feed substrate” [5] .

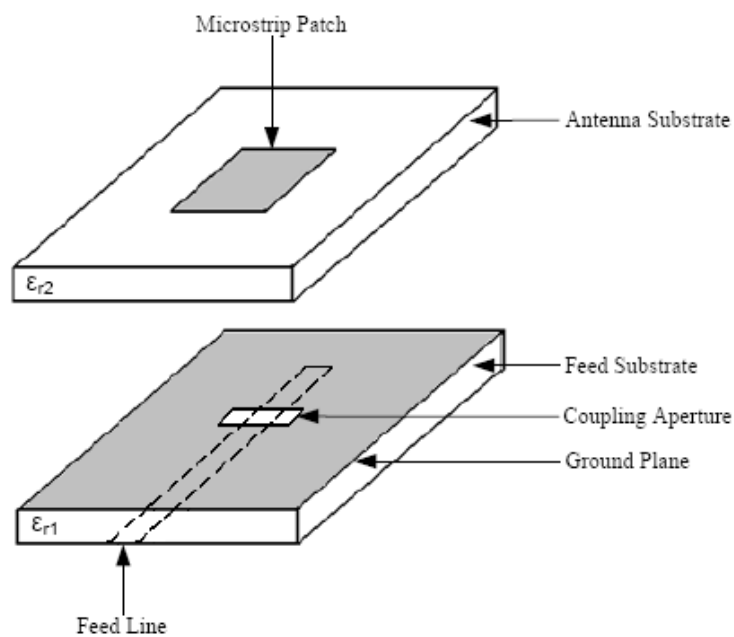


Figure 2-6 Aperture Coupling Feed [5].

The general parameters of “the aperture coupled microstrip patch antenna” are described within this part.

- Antenna substrate dielectric constant:

It is preferred to mount the antenna elements on a low dielectric constant substrate to increase the bandwidth, the radiation efficiency and the range of angle at which scan blindness occurs [23].

- Antenna substrate thickness:

Bandwidth and coupling level are affected from the substrate thickness. As the thickness of the substrate increases, wider bandwidth, and less coupling for a given aperture size is obtained [24]. Microstrip patch antenna should have a thicker substrate and lower permittivity, for better radiation and a higher frequency bandwidth. Neglecting the surface waves, increasing the height of the microstrip patch antenna substrate provides efficiency as large as 90% and bandwidth increases up to 35% [4].

- Microstrip patch length:

The resonant frequency of the antenna is mainly determined by the length of the patch.

- Microstrip patch width:

“The resonant resistance of the antenna is affected by the width of the patch. Lower resistance can be achieved with a wider patch. If dual or circular polarization is required, square patches should be chosen [20].”

- Feed substrate dielectric constant:

Microstrip feed line should have higher permittivity. However, very high permittivity results in great losses because of the increasing value of dielectric loss tangent coefficient. As permittivity of the feed substrate increases, more losses start to occur; feed lines become less efficient and have smaller bandwidth. “Feed substrate dielectric constant should be selected in the range of 2 up to 10 [20].”

- Feed substrate thickness:

Microstrip feed line should have a thinner substrate to ensure proper transmission along microstrip lines. Feed substrate thickness should be in the range of 0.01λ to 0.02λ in order to decrease the spurious radiation from feed lines.

- Feed line width:

“Feed line width controls the characteristic impedance of the feed line[20].”

- Feed line position relative to slot:

“Feed line should be located at right angles to the center of the slot to achieve maximum coupling [20].”

- Position of the patch relative to the slot:

The patch should be centered over the slot for maximum coupling. “Moving the patch relative to the slot in the E-plane (resonant) direction will decrease the coupling level [24].”

- Length of the tuning stub

“Length of the tuning stub is the distance between the edge of the open-ended transmission line and the center of the aperture. The tuning stub is used to tune the excess reactance of the slot coupled antenna. The stub is generally less than $\lambda_g/4$ in length. The effect of the stub length is to rotate the entire impedance locus up (inductive) or down (capacitive) on the Smith chart [20]. Adjusting the slot length and the stub length, optimum matching condition can be achieved.”

CHAPTER 3

DESIGN OF APERTURE COUPLED PATCH ANTENNAS

There are three sections of this chapter which involves parametric analysis of rectangular and H-shaped aperture coupled microstrip antennas and the design of dual polarized antenna. In the first section, rectangular aperture coupled antenna is investigated with resonant frequency at 2.21GHz. The parametric analysis is done for each variable. In the second section, design of an H-shaped aperture coupled patch antenna is realized at the same frequency. Same bandwidth and return loss characteristics are shown to be obtained with smaller H-shaped slot.

Parametric analysis of H-shaped slot coupled patch antenna is also studied to get the optimum bandwidth and return loss characteristics. In the third section of this chapter, “the design of dual polarized aperture coupled antenna with two H-shaped slots” are realized.

3.1 Parametric Analysis of Rectangular Aperture Coupled Microstrip Patch Antenna

Design, analysis and simulation results obtained for rectangular slot coupled microstrip antenna at 2.21GHz will be presented, with the evaluation of various parameters' effects on the optimization of design. The parameters are analyzed one by one, with the particular effect on antenna performance, within the next subsections. The dielectric constant values and the thicknesses of the dielectric

materials used throughout the parametric analysis is as in Figure 3-1. Table 3-1 and Figure 3-2 shows the antenna design parameters

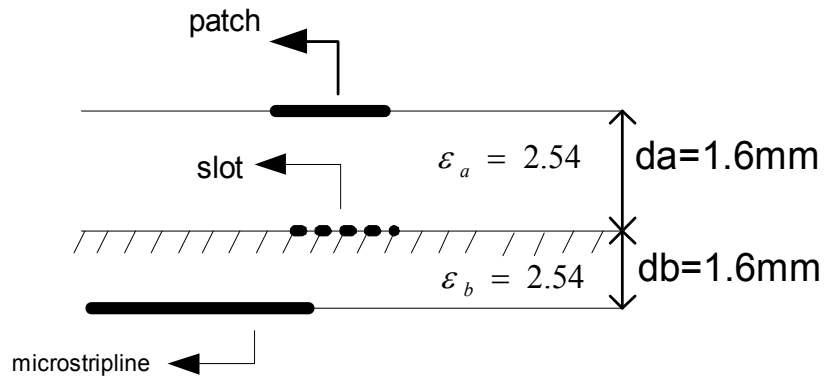


Figure 3-1 Substrate parameters.

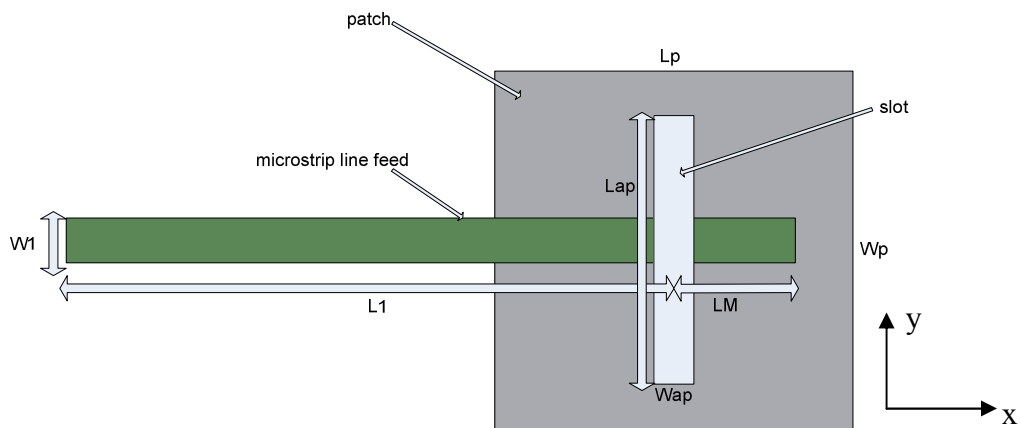


Figure 3-2 Antenna structure with corresponding design parameters.

Table 3-1 Design parameters of rectangular slot coupled microstrip patch antenna at 2.21GHz.

| Design Parameter | Value |
|--------------------------------------------------------------------------------|--------|
| L_p = Patch Length | 40mm |
| W_p = Patch Width | 30mm |
| W_{ap} = Width of rectangular aperture | 1.55mm |
| L_{ap} = Length of rectangular aperture | 11.2mm |
| L_1 = Microstrip feedline length | 58mm |
| W_1 = Microstrip feedline width | 4.42mm |
| x_{of} = offset in x direction (resonance direction) | 0mm |
| y_{of} = offset in y direction (direction orthogonal to resonance direction) | 0mm |
| LM = Stub length | 20mm |

3.1.1 Analysis of Stub Length Effects to the Antenna Performance

In this subsection, the variation of antenna input impedance with respect to the stub length changes is investigated. To understand stub length effects, parametric analysis has been performed and result of parametric analysis is presented as the return loss and bandwidth characteristics using the Smith Chart and return loss graphs (S_{11}). For increasing length of stub from 4mm to 20mm, the results in Figure 3-3, Smith Chart and Figure 3-4, rectangular plot are observed.

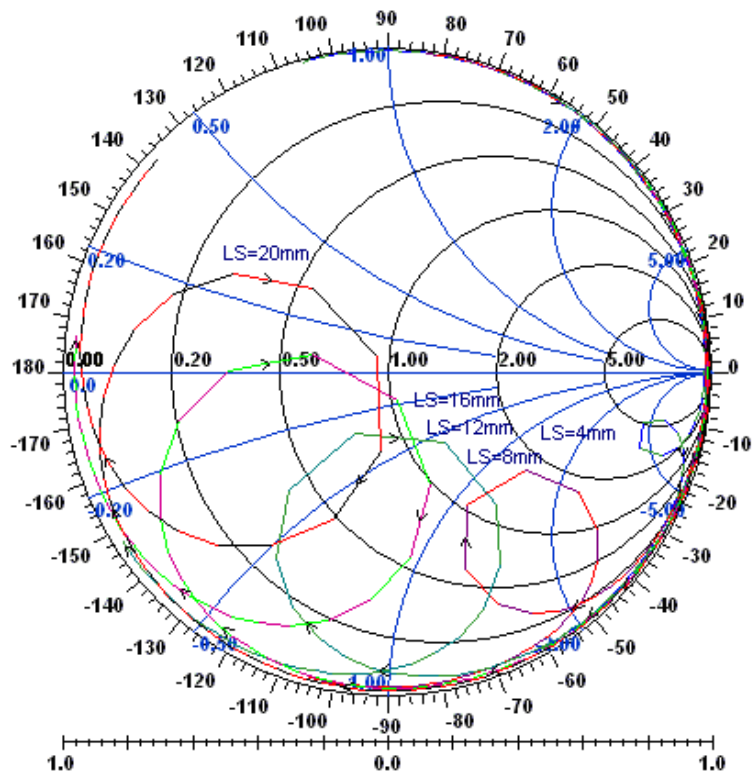


Figure 3-3 Input impedance as a function of stub length.

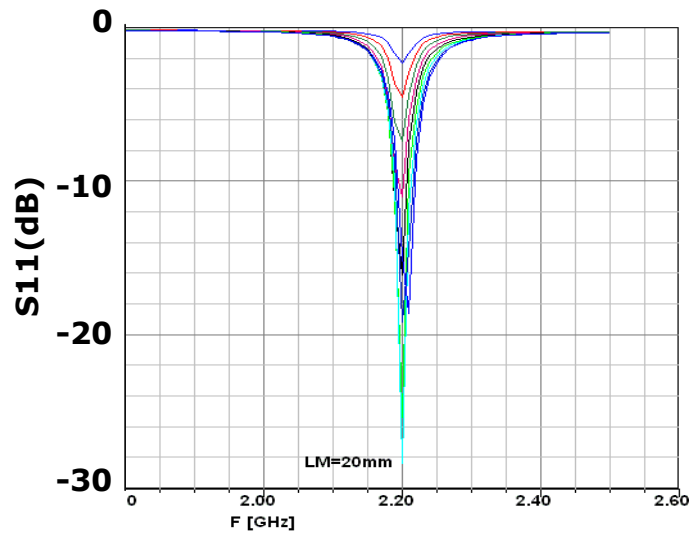


Figure 3-4 S_{11} as a function of stub length.

3.1.2 Analysis of Slot Length Effects to the Antenna Performance

In this section, antenna input impedance with respect to the slot length changes is investigated. The varying parameter is the slot length L_{slot} , which is changed from 8mm to 14mm.

As shown in Figure 3-6 and Figure 3-7, “the decreasing aperture length decreased the radius of the impedance circle and the center of the circle moved to the short circuit location” as also mentioned in [22]. This is related with “the decreasing coupling factor between the feedline and the patch antenna” [22].

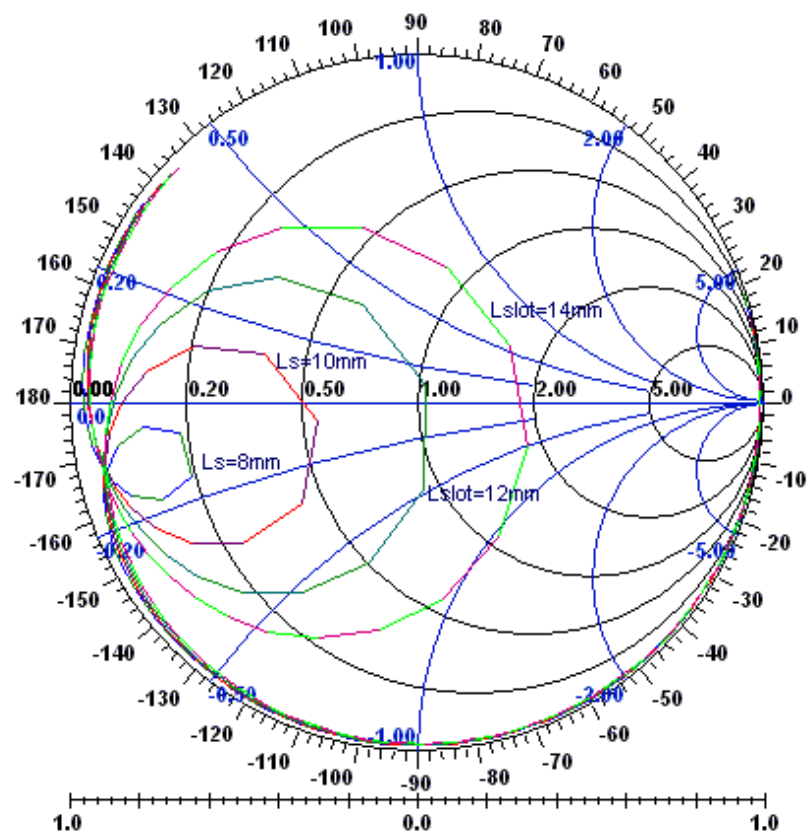


Figure 3-6 Antenna input impedance as a function of slot length.

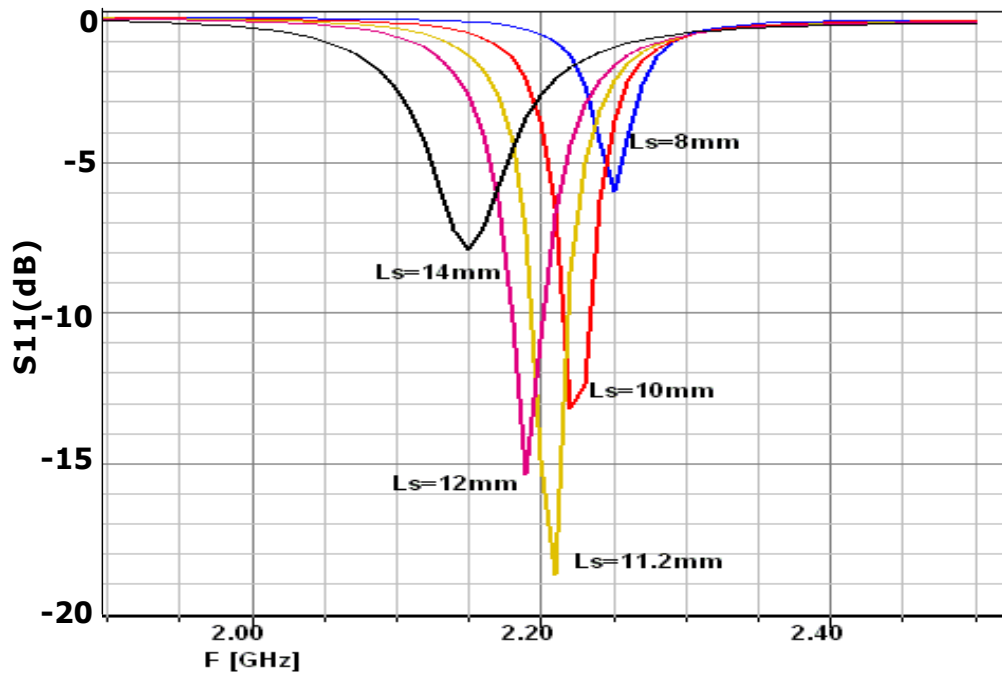


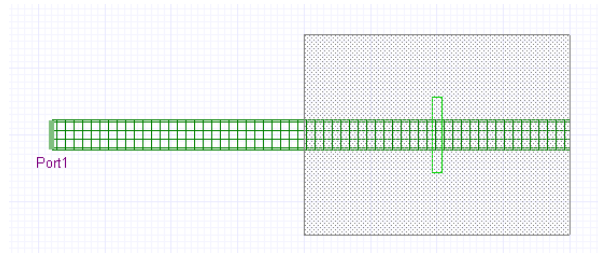
Figure 3-7 Calculated input impedance as a function of aperture length.

It is deduced that, “the required resistive part of the impedance of the antenna can be obtained by the adjustment of slot length” [22]. Similarly, required reactance of the impedance can be obtained by adjusting stub length. Also slot length affects the resonant frequency. “Decreasing the slot length has an increasing effect on the resonant frequency of the antenna and increasing the slot length has a decreasing effect on the resonant frequency of the antenna” [22] as seen in Figure 3-7. This effect of the slot length can be utilized for optimizing antenna parameters to reach the desired resonance frequency.

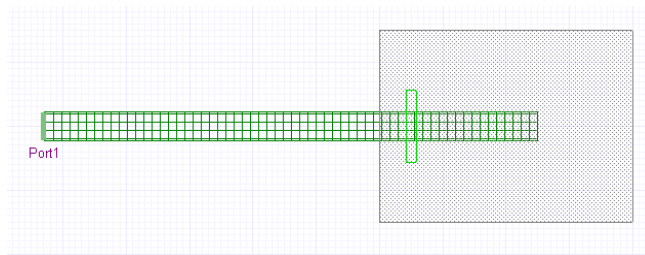
3.1.3 Patch Position Effects to the Antenna Performance

In this section, antenna input impedance with respect to the patch position changes is investigated. The varying parameters are offset values, x_{of} and y_{of} , which are

changed from 0mm to 15mm one by one. For changes in offset value in x direction the alternative structures are given in Figure 3-8.



a) $x_{of}=0\text{mm}$



b) $x_{of}=15\text{mm}$

Figure 3-8 View of the antenna structure for different values of x_{of} .

The simulation results for x_{of} from 0mm to 15 mm are provided in Figure 3-9 and Figure 3-10. The input impedance is sensitive to large variations in patch position over the slot, but not too much sensitive to the small variations in patch offsets. Since “magnetic field distribution under the patch is a half sinusoid with a peak at the center, the coupling is maximum when the slot is at the center of the patch and decreases as the slot moves towards the edges” [4]. This can be observed from the changes in the radius of the impedance loci. “With increasing offset, the centers of

the resonant loops move nearly in a straight line toward the edge of the Smith Chart to the inductive side of the short position. Similar behavior was also observed for decreasing slot length, since both the size and position of the slot affect the amount of coupling. On the other hand, the offset value in x direction has not serious but noteworthy effect on the resonant frequency of the antenna.[22]”

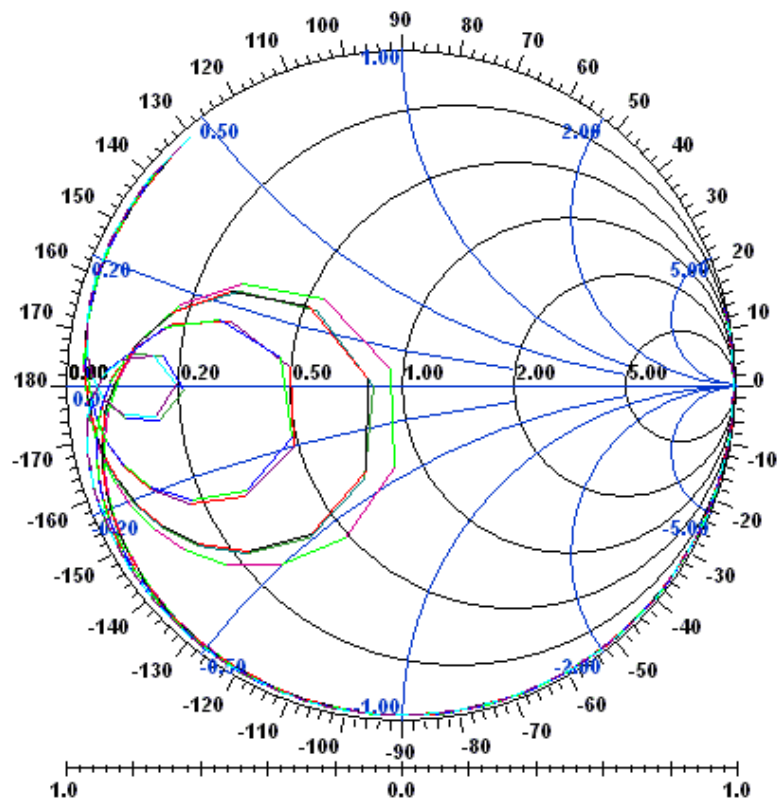


Figure 3-9 Effect of x_{of} on input impedance loci.

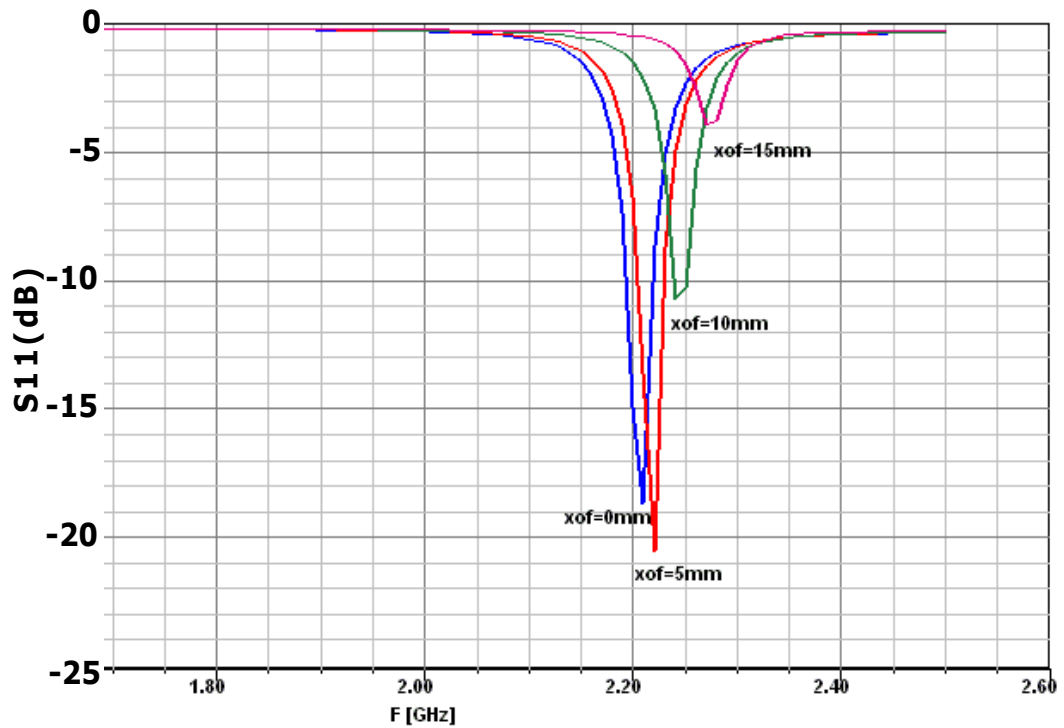
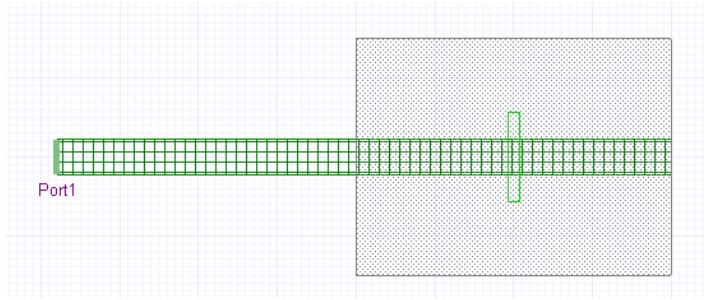
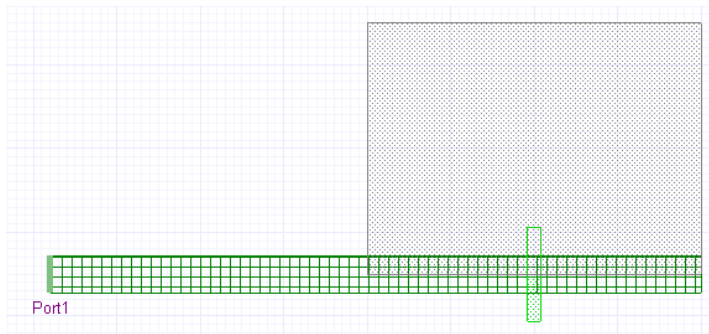


Figure 3-10 Effect of xof on input return loss.

However, “movement of the patch in the y-direction causes smaller change in the coupling factor as long as the slot remains under the patch” [22]. For changes in offset value in y direction the alternative designs of the structure are given in Figure 3-11.



a) $y_{of}=0\text{mm}$



b) $y_{of}=15\text{mm}$

Figure 3-11 View of the antenna structure for different values of y_{of} .

The results are provided in Figure 3-12 and Figure 3-13. It is observed that offset in y -direction does not have any significant effect on the antenna performance as long as the slot completely remains under the patch, since the field under the patch does not change in y -direction for this mode of the cavity. As expected the amount of coupling decreases when some part of the slot moves outside of the patch.

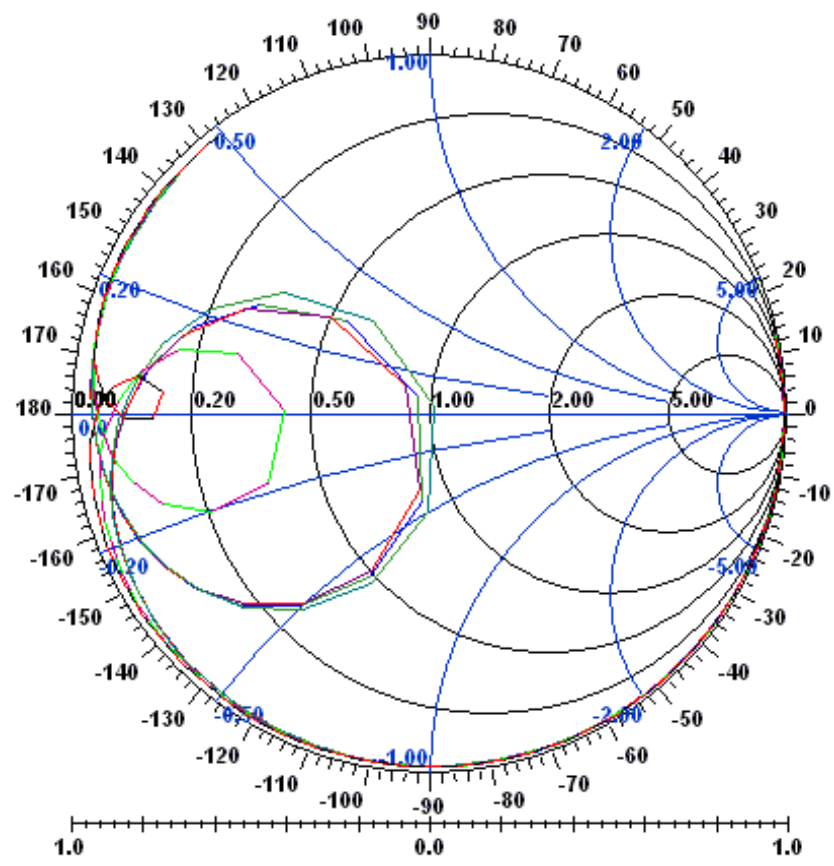


Figure 3-12 Effect of y_{of} on input impedance.

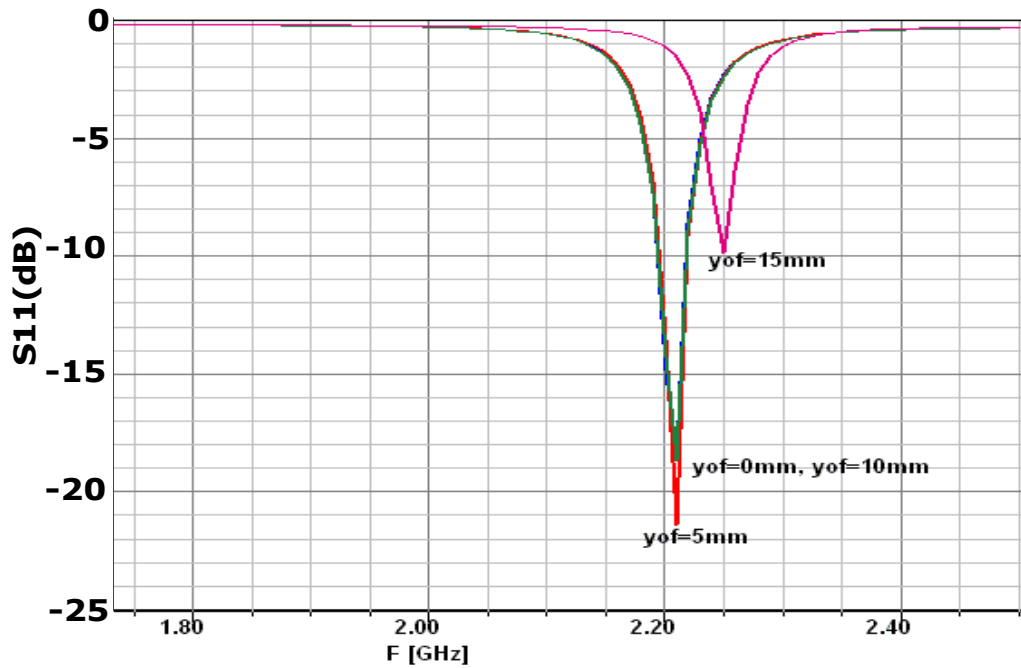
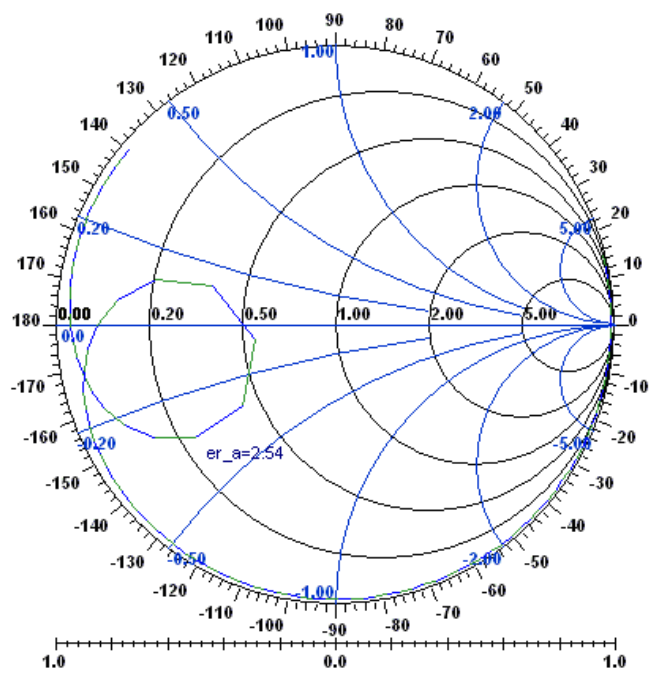


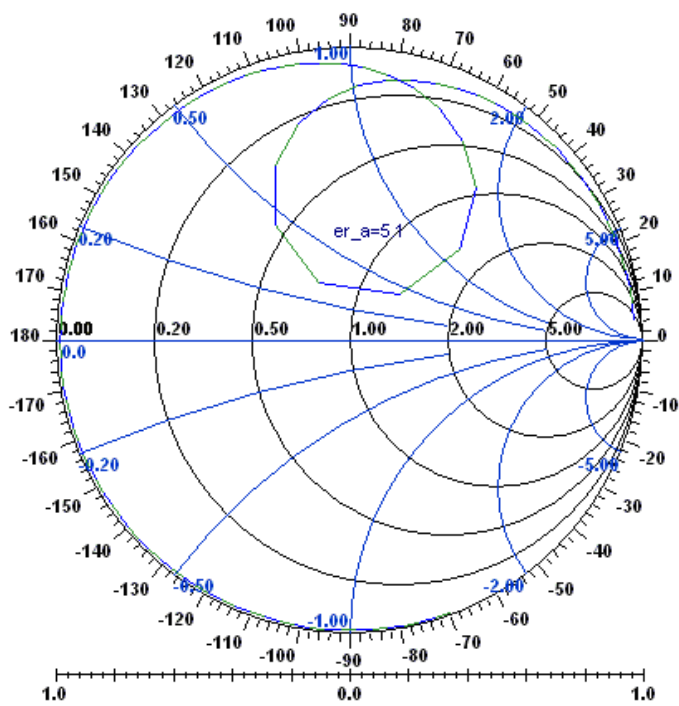
Figure 3-13 Effect of y_{of} on input return loss.

3.1.1 Effect of permittivity and the thickness of the antenna substrate to the antenna performance

The effect of ϵ_a and d_a on the antenna input impedance is analyzed. Varying parameters are the antenna substrate dielectric constant $\epsilon_a=2.54, 3.38$ and $d_a=1.6\text{mm}, 3.2\text{mm}$ and 4.8mm . The results are provided in Figure 3-14 and Figure 3-15.



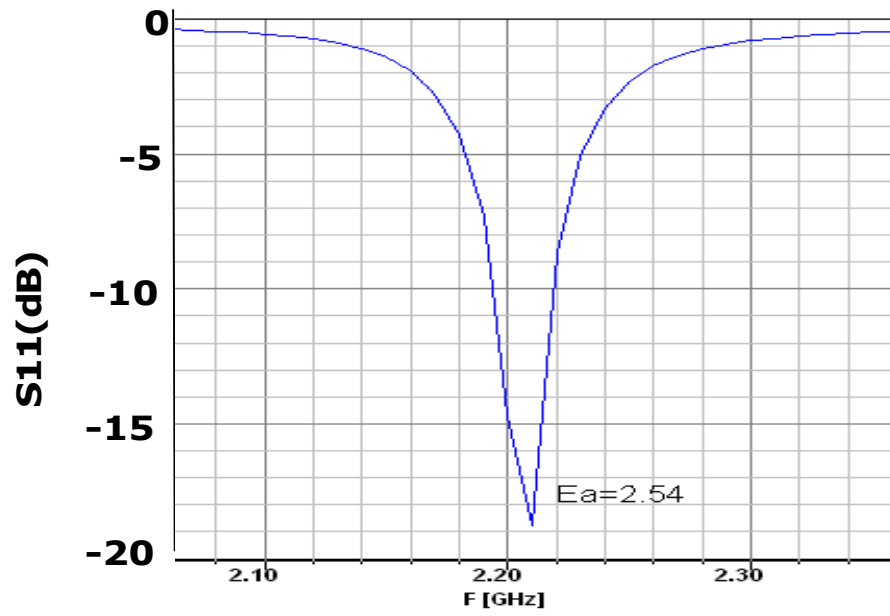
a)



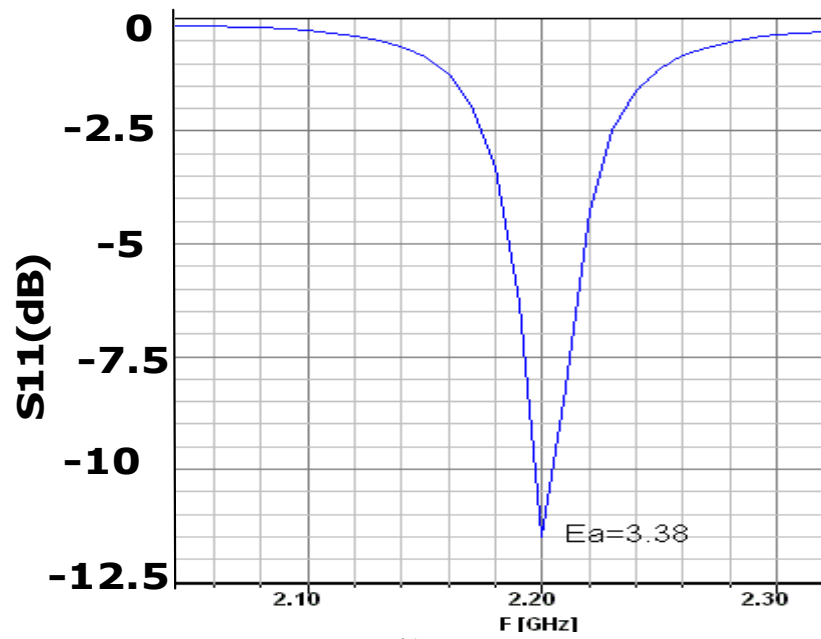
b)

Figure 3-14 Effect of the permittivity of the antenna substrate for different ϵ_a values

a) $\epsilon_a=2.54$, b) $\epsilon_a=3.38$.



a)

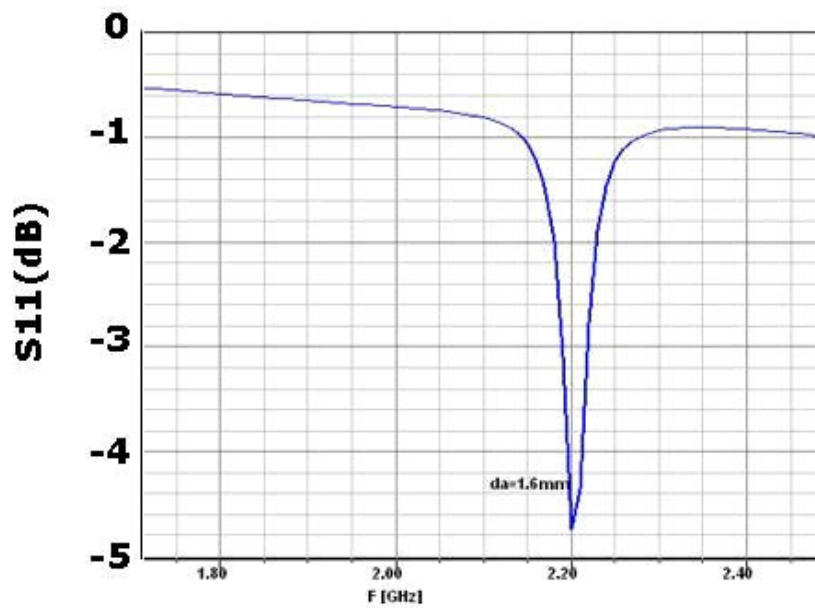


b)

Figure 3-15 Return loss graph for different values of ϵ_a a) $\epsilon_a = 2.54$, b) $\epsilon_a = 3.38$.

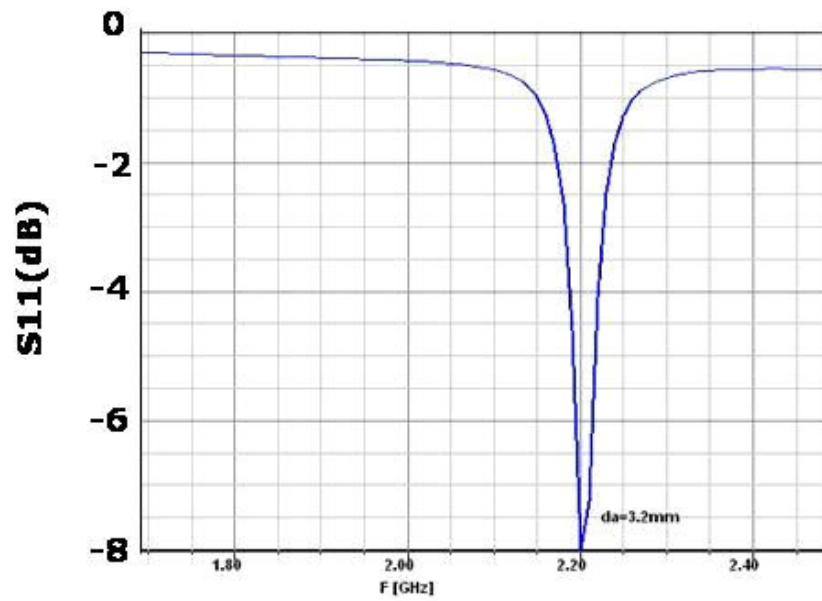
From the simulation results “the resonant frequency of the antenna is not affected from the changes in antenna substrate dielectric constant” [22]. Increasing antenna substrate dielectric constant has an adverse effect on return loss characteristics and radiation efficiency.

Next, the varying parameter is the antenna substrate thickness which is changing as 1.6mm, 3.2mm and 4.8mm. As the distance between the radiating patch and slot increases, better radiation and a higher frequency bandwidth as depicted in Figure 3-16.

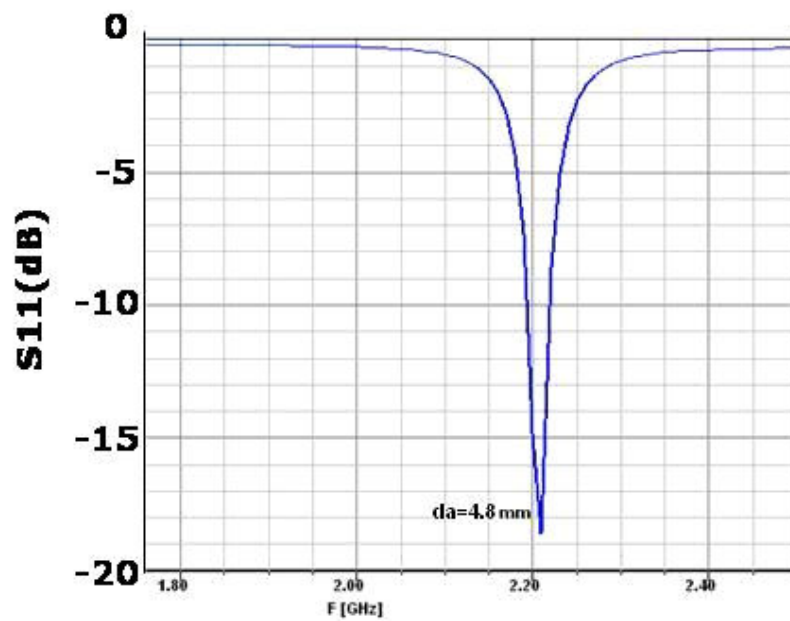


a)

Figure 3-16 Return loss graph for different values of the thickness of the feed substrate; a) $d_a=1.6$ mm, b) $d_a=3.2$ mm, c) $d_a=4.8$ mm.



b)



c)

Figure 3-17 Return loss graph for different values of the thickness of the feed substrate; a) $d_a=1.6$ mm, b) $d_a=3.2$ mm, c) $d_a=4.8$ mm. (Continued)

From the simulation results “it is observed that the resonant frequency of the antenna is not affected from the changes in antenna substrate thickness in similarity

with dielectric constant variations of the antenna substrate” [22]. Increasing antenna substrate thickness satisfies better frequency bandwidth and radiation characteristics.

3.2 Parametric Analysis of H-Shaped Slot Coupled Microstrip Patch Antenna

In this section of the thesis, it is aimed to reach to the return loss and radiation pattern characteristics of a rectangular slot with a smaller size H-shaped slot. The rectangular slot is replaced with an H-shaped slot and parametric analysis for the optimum size of the H-shaped slot is realized. The design parameters of H-shaped slot coupled microstrip patch antenna are shown in Figure 3-18.

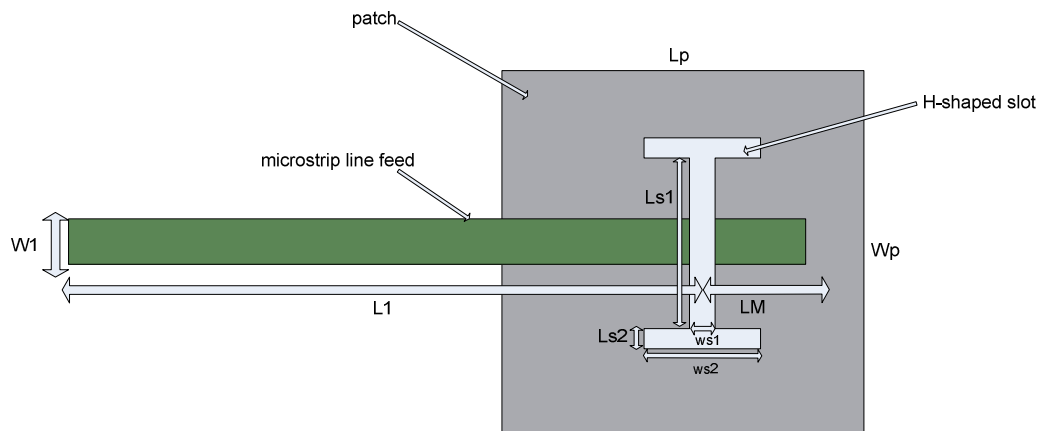


Figure 3-18 Microstrip fed “H-shaped slot coupled patch antenna” parameters.

Within the rest of this part, design analysis and simulation results obtained for H-shaped slot coupled microstrip patch antenna will be described, with evaluation of various design parameters on the optimization. The parameters are analyzed one by

one, with the particular affect on antenna performance. Antenna design parameters are listed in Table 3-2 with the fixed optimized values. Within the analysis of the effects, each parameter will be adjusted and the respective results will be described.

Table 3-2 Design parameters of H-shaped slot coupled microstrip patch antenna at 2.21GHz.

| Design Parameter | Value |
|--------------------------------------------------------|--------|
| L_p = Length of the patch | 40mm |
| W_p = Width of the patch | 30mm |
| ls1=length of H slot center leg | 6mm |
| ws1=width of H slot center leg | 1.55mm |
| ls2=length of H slot side leg | 1.55mm |
| ws2=width of H slot side leg | 4mm |
| L_1 = Microstrip feedline length | 58mm |
| W_f = Microstrip feedline width | 4.42mm |
| x_{of} = offset in x direction (resonance direction) | 0mm |
| y_{of} =offset in y direction (resonance direction) | 0mm |
| LM = Stub length | 20mm |

3.2.1 Analysis of Stub Length Effects to the Antenna Performance

In this section, antenna input impedance with respect to the stub length changes is investigated. For increasing length of stub from 4mm to 20mm, the results in Figure 3-19 and Figure 3-20 are observed.

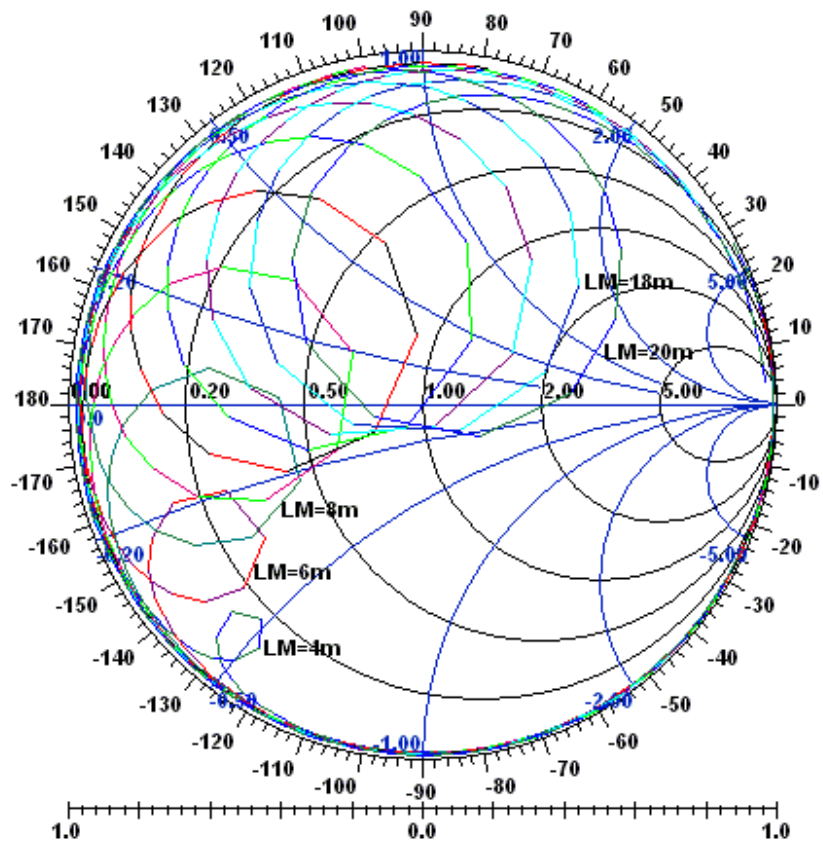


Figure 3-19 Input impedance as a function of stub length.

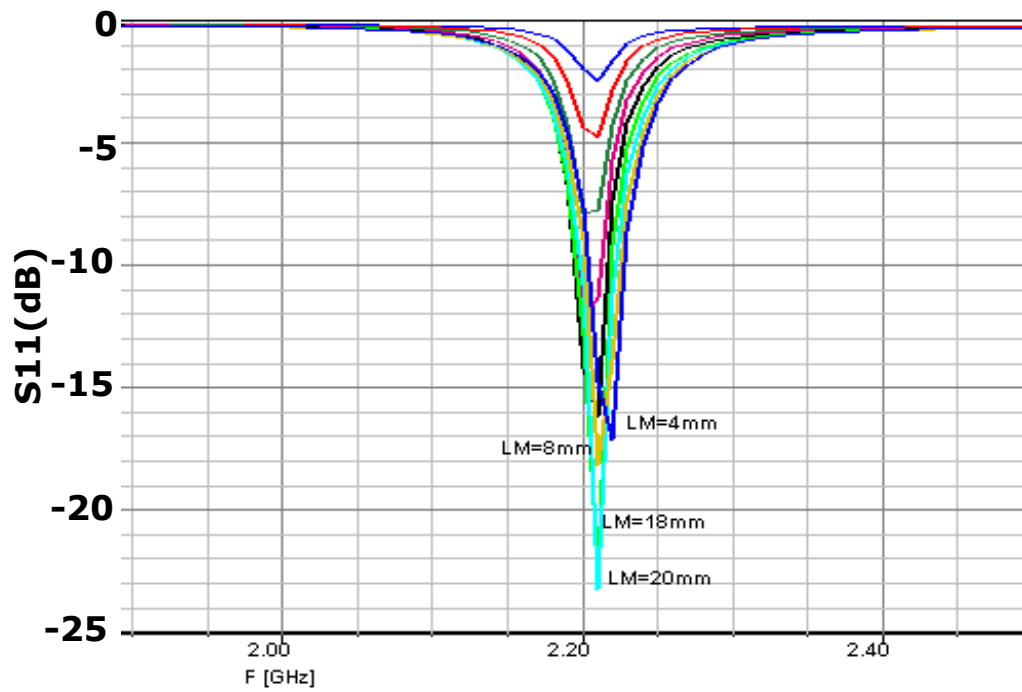


Figure 3-20 S11 as a function of stub length LM from 4mm to 20mm.

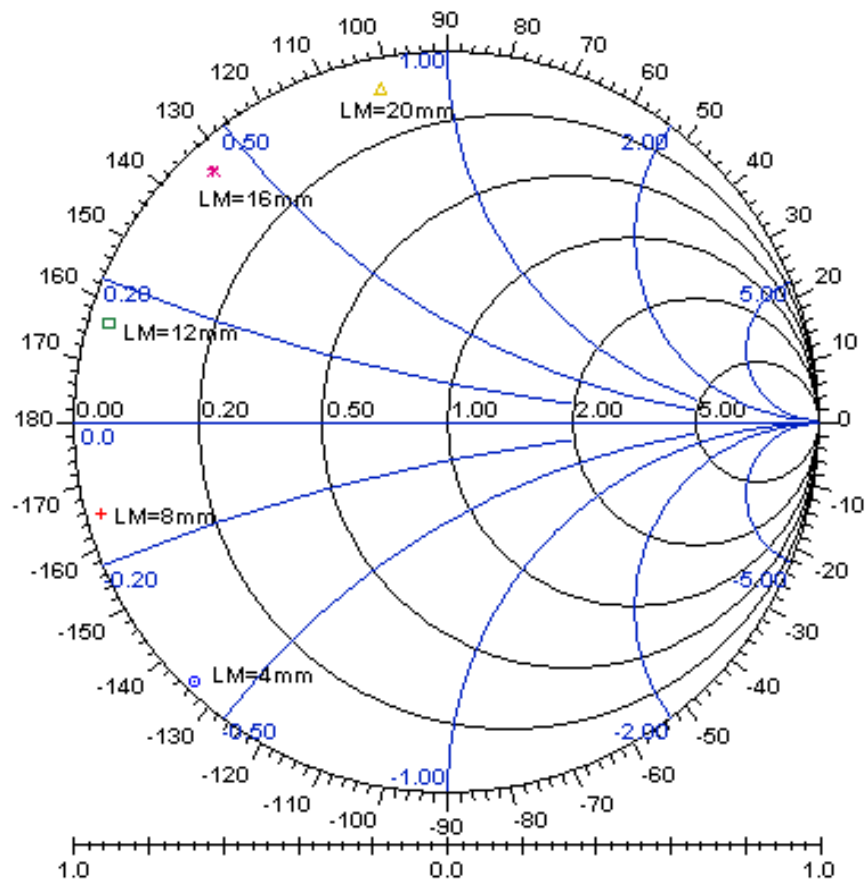


Figure 3-21 Input impedance at a single frequency for different values of the stub length ($f=2.21\text{MHz}$).

The input impedance at a single frequency (2.21MHz) is plotted for different values of stub length in Figure 3-21. A resistance contour is obtained with a constant value similar to rectangular slot case. From Figure 3-20, it is deduced that “increasing the value of the stub length has a reducing effect on the resonance frequency and bandwidth of the antenna” [22].

3.2.2 Analysis of H-Shaped Slot Dimensions to the Antenna Performance

3.2.2.1 Analysis of Length of Center Arm

In this section, antenna input impedance with respect to the H-shaped slot center arm length changes is investigated. The varying parameter is the length of the center arm, l_{s1} , which is changed from 4mm to 12mm. Figure 3-22 and Figure 3-23 depicts the simulation results. As l_{s1} is reduced, “the radius of the impedance circle decreases and the center of the circle moves to the short circuit location” [22]. This might be due to the decrease in the coupling factor between the feed line and the patch antenna. Also the resonant frequency decreases as l_{s1} increases.

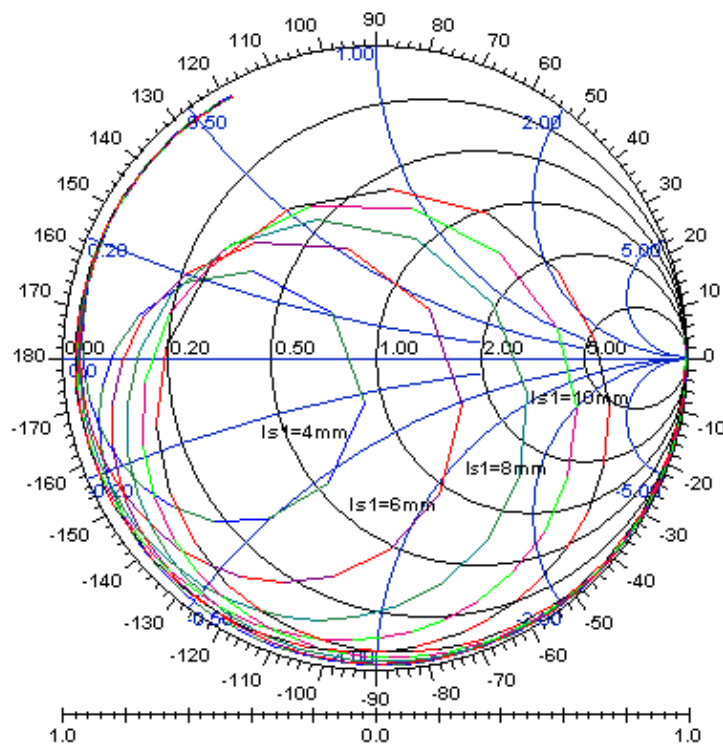


Figure 3-22 Input impedance as a function of l_{s1} .

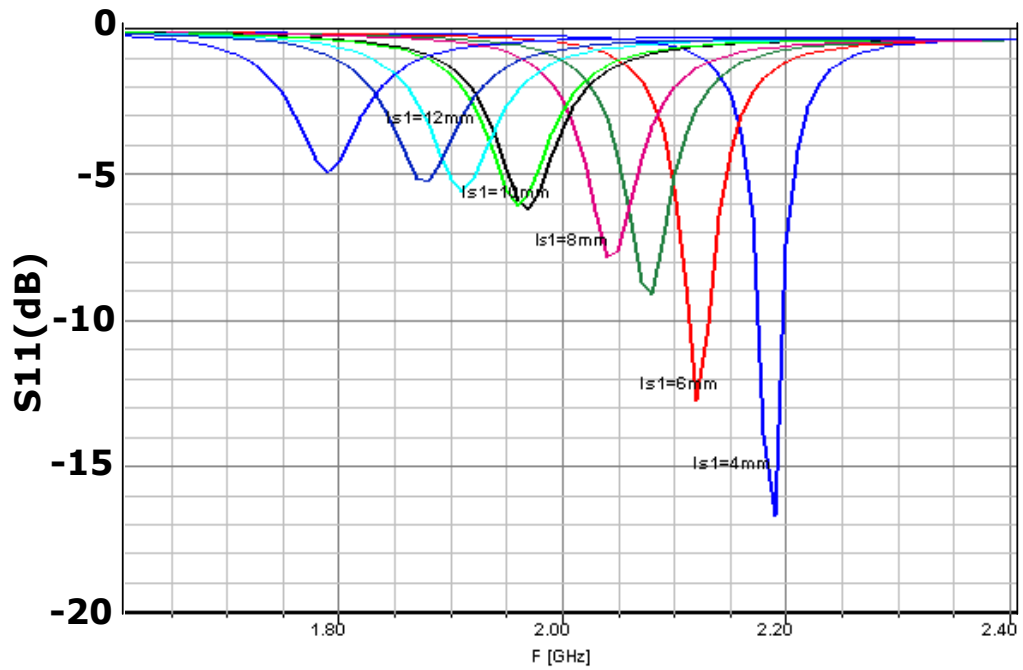


Figure 3-23 Return loss as a function of l_{s1}

3.2.2.2 Analysis of Length of Side Legs

In this section, antenna input impedance with respect to the length of side legs of H-shaped slot is investigated. The varying parameter is ws_2 , which is changed from 4mm to 12mm. The simulation results are plotted in Figure 3-24 and Figure 3-25.

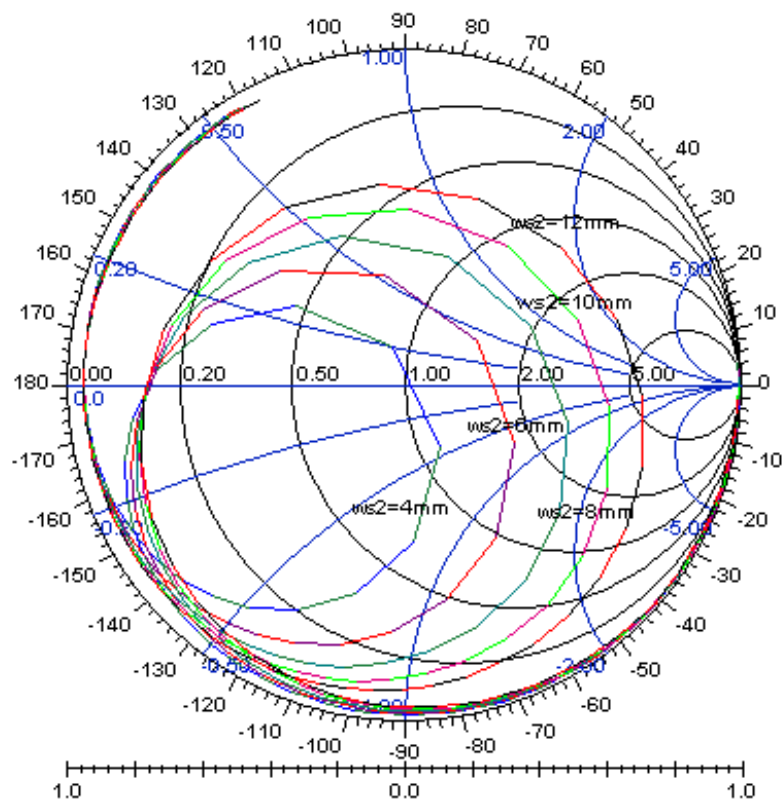


Figure 3-24 Input impedance as a function of ws_2 .

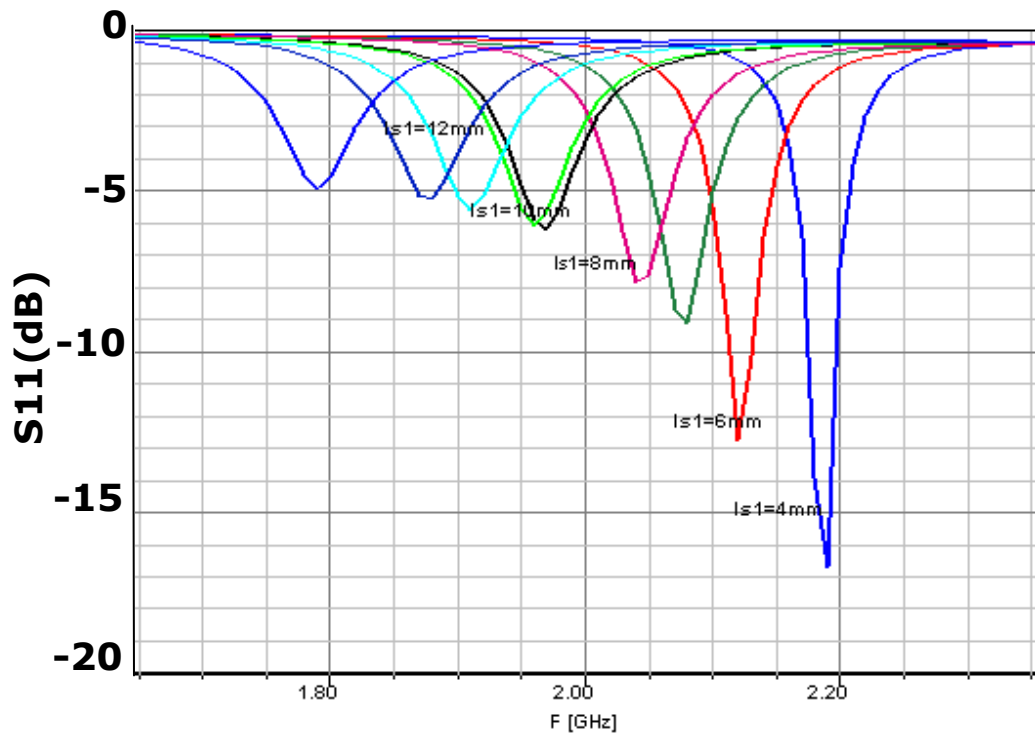


Figure 3-25 Return loss as a function of ws_2 .

It is understood that, “the effects of ws_2 on the input impedance locus and on the resonance frequency of the antenna are same as the effects of l_{s1} ” [22]. Hence, for the H-shaped aperture there is an additional parameter compared to rectangular aperture that can be utilized to optimize the resonance frequency and input impedance of the antenna.

3.2.3 Patch Position Effects to the Antenna Performance

For increasing offset in x direction (x_{of}) from 0mm to 15mm, the simulation results are presented by Figure 3-26, Figure 3-27.

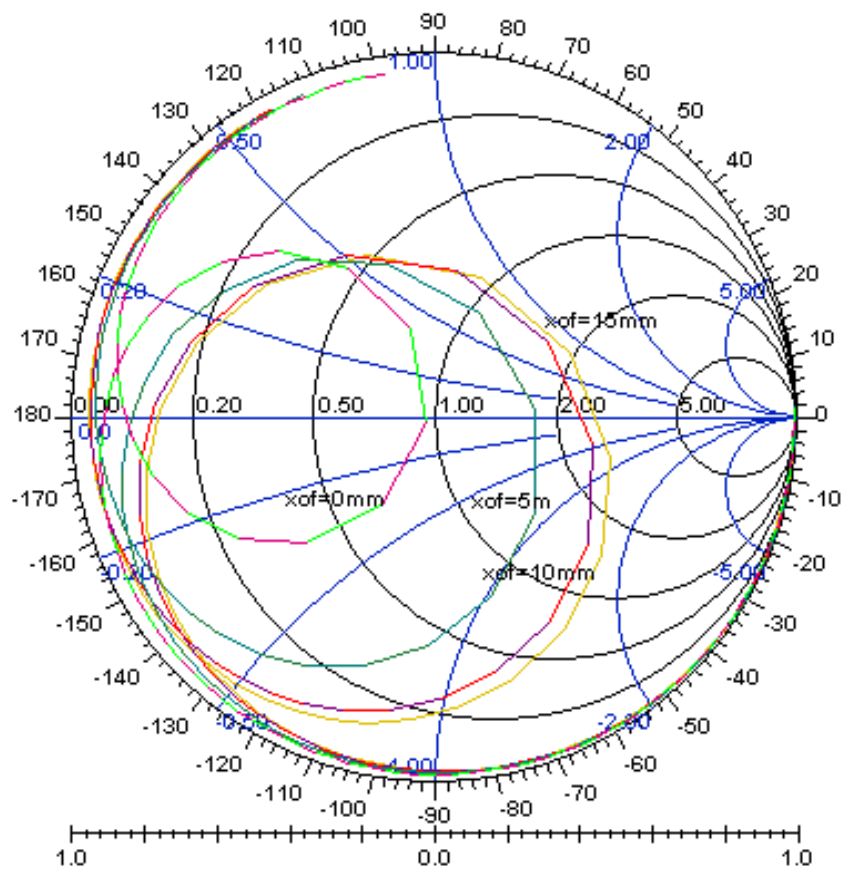


Figure 3-26 Effect of x_{of} on input impedance

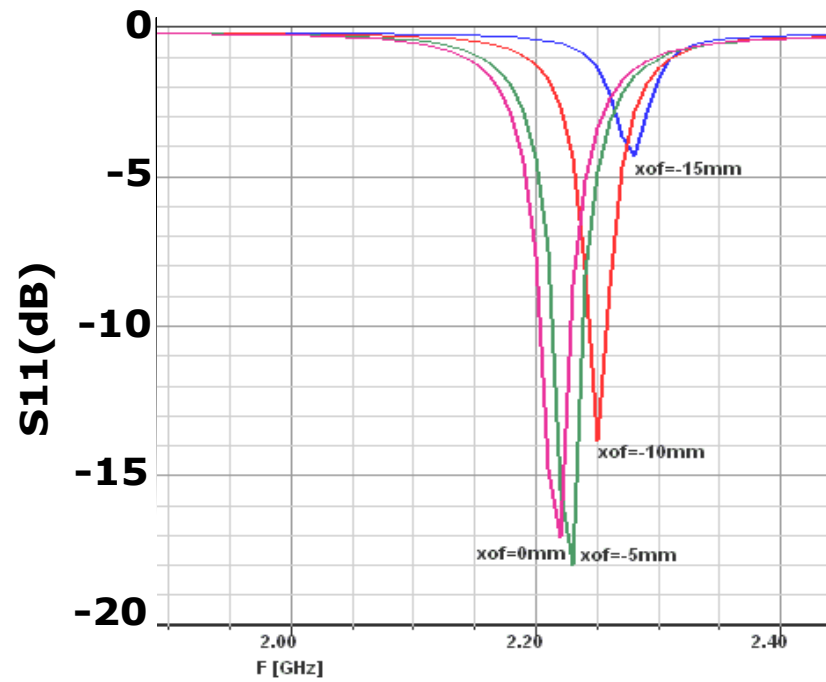


Figure 3-27 Effect of xof on input return loss.

Figure 3-27 shows that “return loss response” is optimum when $x_{of}=0\text{mm}$ and increasing the offset value for H-shaped slot has an “increasing effect on resonant frequency”.

Figure 3-28, Figure 3-29 are results of simulation for varying parameter y_{of} for the H-shaped slot.

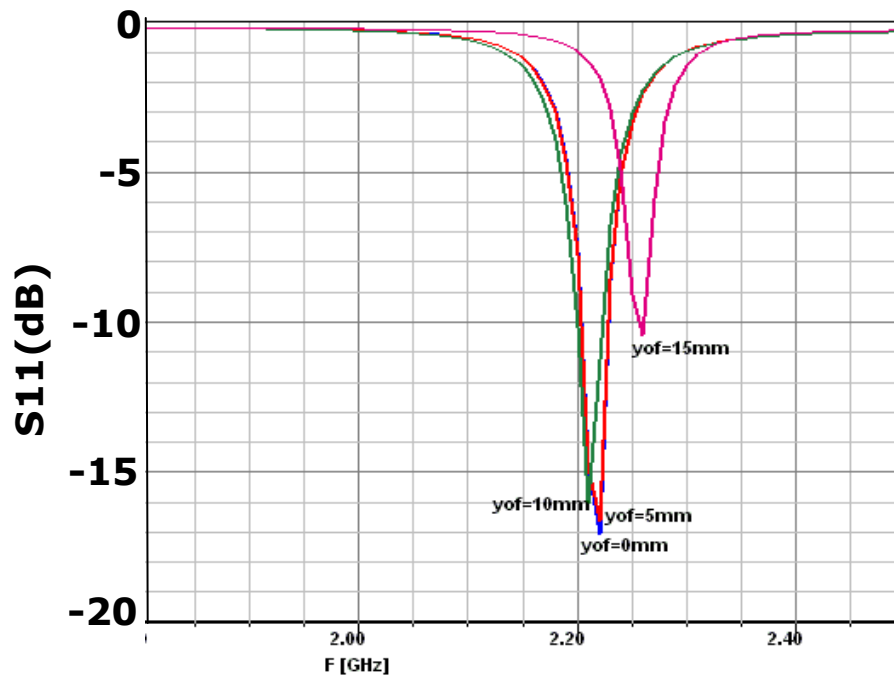


Figure 3-29 Effect of the patch position to input impedance.

Offset value in y (nonresonant) direction has a smaller effect on the coupling amount and input impedance with respect to the offset value in x (resonant) direction.

The optimum dimensions of the apertures for rectangular and H-shaped slots reached at the end of parametric analysis are given in Figure 3-30 in order to be able to make a size comparison.

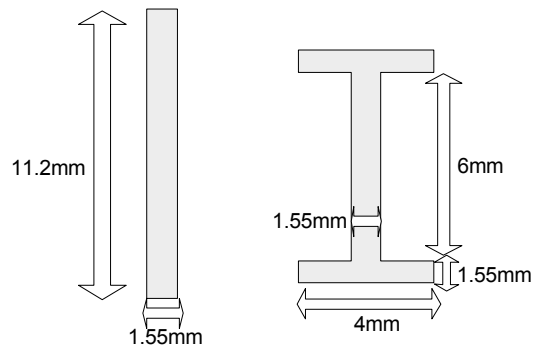
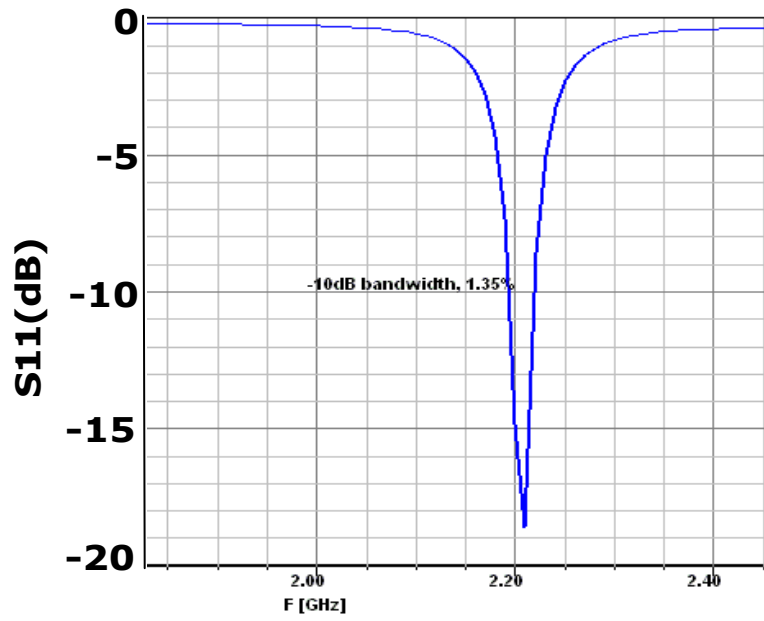
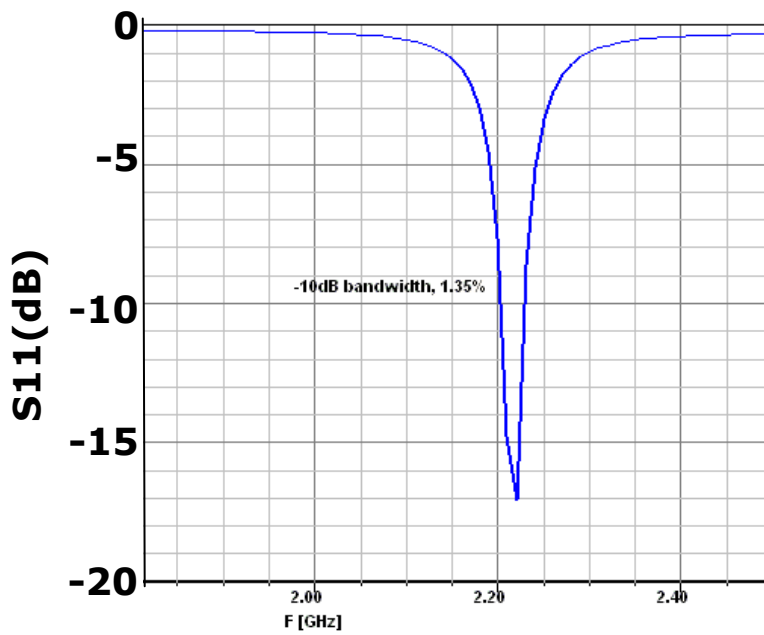


Figure 3-30 Sizes of the rectangular slot and H-shaped slot at 2.21GHz.

The bandwidth characteristics of rectangular slot coupled microstrip patch antenna and H-shaped slot coupled patch antenna with optimized design parameters are shown in Figure 3-31. It is observed that the same bandwidth response can be obtained with a shorter but wider H-shaped slot compared to a rectangular slot.



a)



b)

Figure 3-31 Return loss graphs of a) rectangular slot, b) H-shaped slot coupled patch antennas.

The radiation patterns of rectangular and H-shaped slot coupled antennas are also compared at 2.21 GHz. “E and H plane radiation patterns for co-polar and cross-polar components of the electric field” are presented in Figure 3-32 for rectangular and in Figure 3-33 for H-shaped antenna.

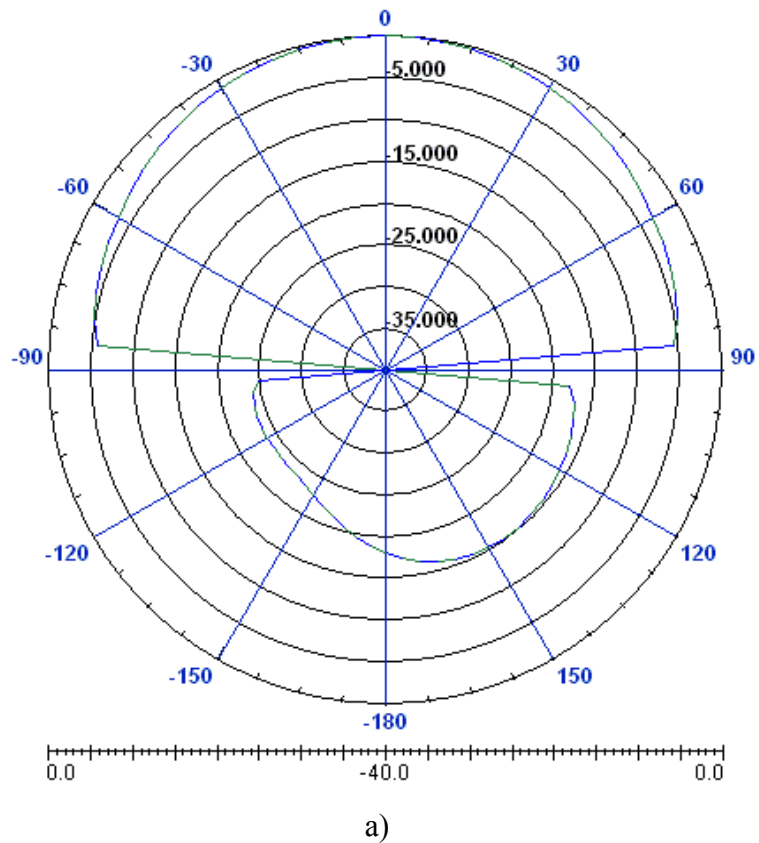
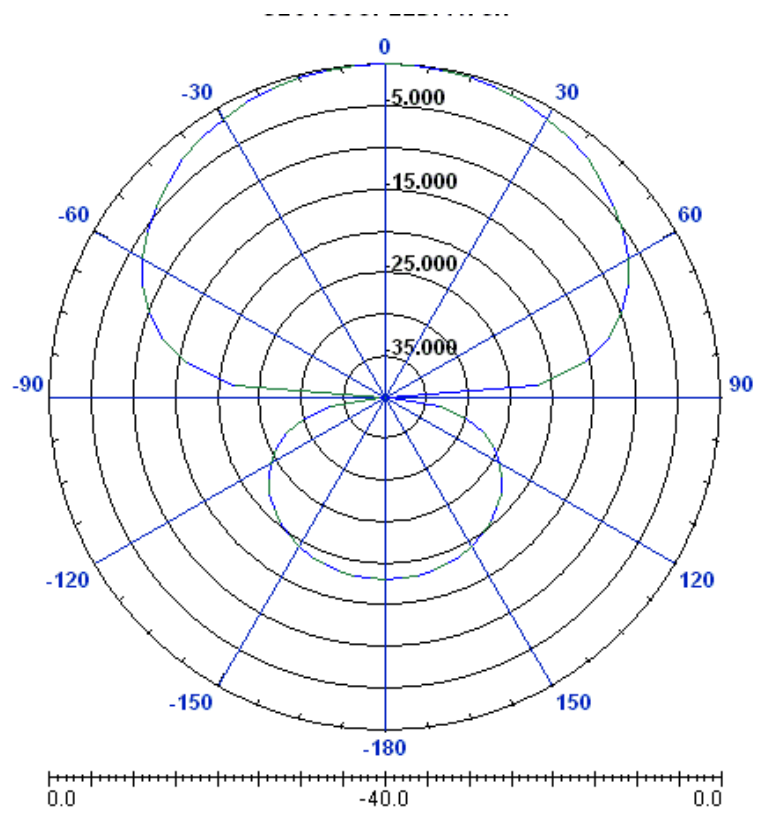


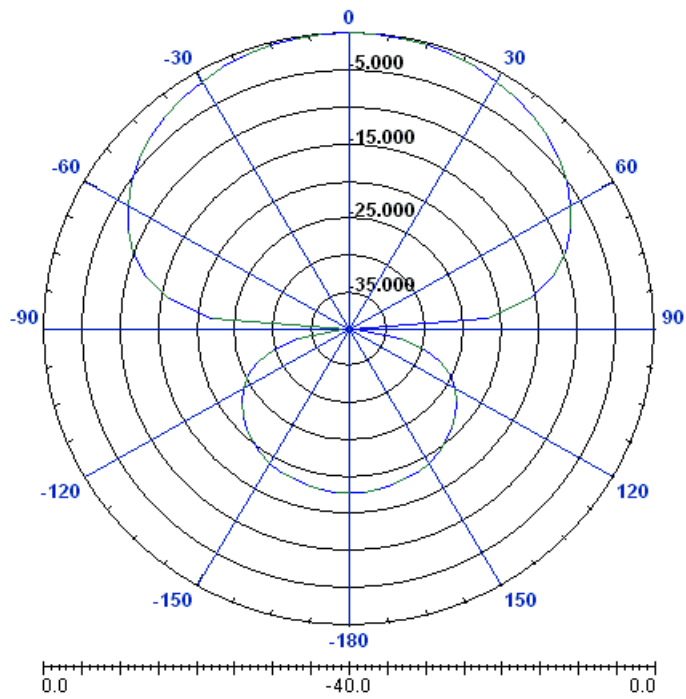
Figure 3-32 Radiation characteristics of rectangular slot coupled patch antenna
a) E-plane, b) H-plane.



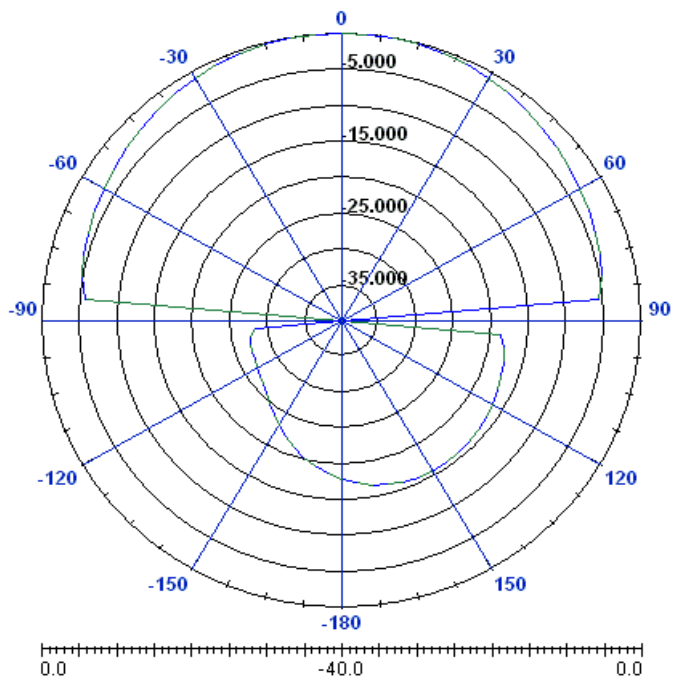
b)

Figure 3-32 Radiation characteristics of rectangular slot coupled patch antenna

a) E-plane, b) H-plane. (Continued)



a)



b)

Figure 3-33 Radiation characteristics of H-shaped slot coupled patch antenna
a) E-plane, b) H-plane

It is observed that radiation pattern characteristics are actually similar for H-shaped slot coupled patch antenna and rectangular slot coupled patch antenna. For rectangular and H-shaped slot coupled patch antenna cross polar levels $< -60\text{dB}$ for each principle plane, therefore they are not shown in the radiation pattern figures.

3.3 Parametric Analysis of Dual Polarized H-Shaped Slot Coupled Microstrip Patch Antenna

In this section the design process of a dual polarized microstrip patch antenna operating in 1710–1880 MHz frequency band will be presented. To achieve this bandwidth, a low dielectric substrate is needed. Foam material with ϵ_r of 1.025 is chosen as antenna substrate. This material is available with a thickness of 7 mm, so two layers of foam is used in order to achieve the required bandwidth. A dielectric is required for supporting patch antenna on foam. The patch antenna is located on bottom layer so that substrate acts like a radome. Parameters of dielectric substrates used for the design are as presented by Figure 3-34.

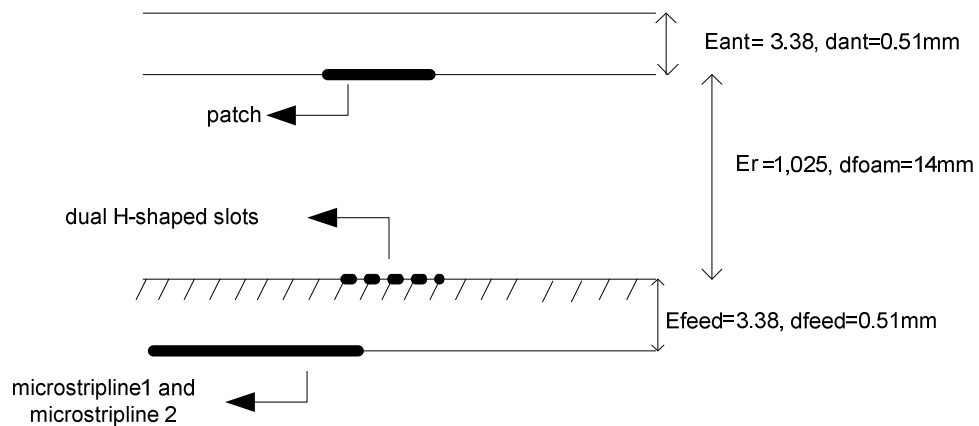


Figure 3-34 Side view of dual H-shaped slot coupled patch antenna structure

The dual polarization operation is obtained by feeding the patch with two H-shaped slots. For maximum isolation, the slots are positioned in a ‘T-shaped’ configuration as presented by Figure 3-35.

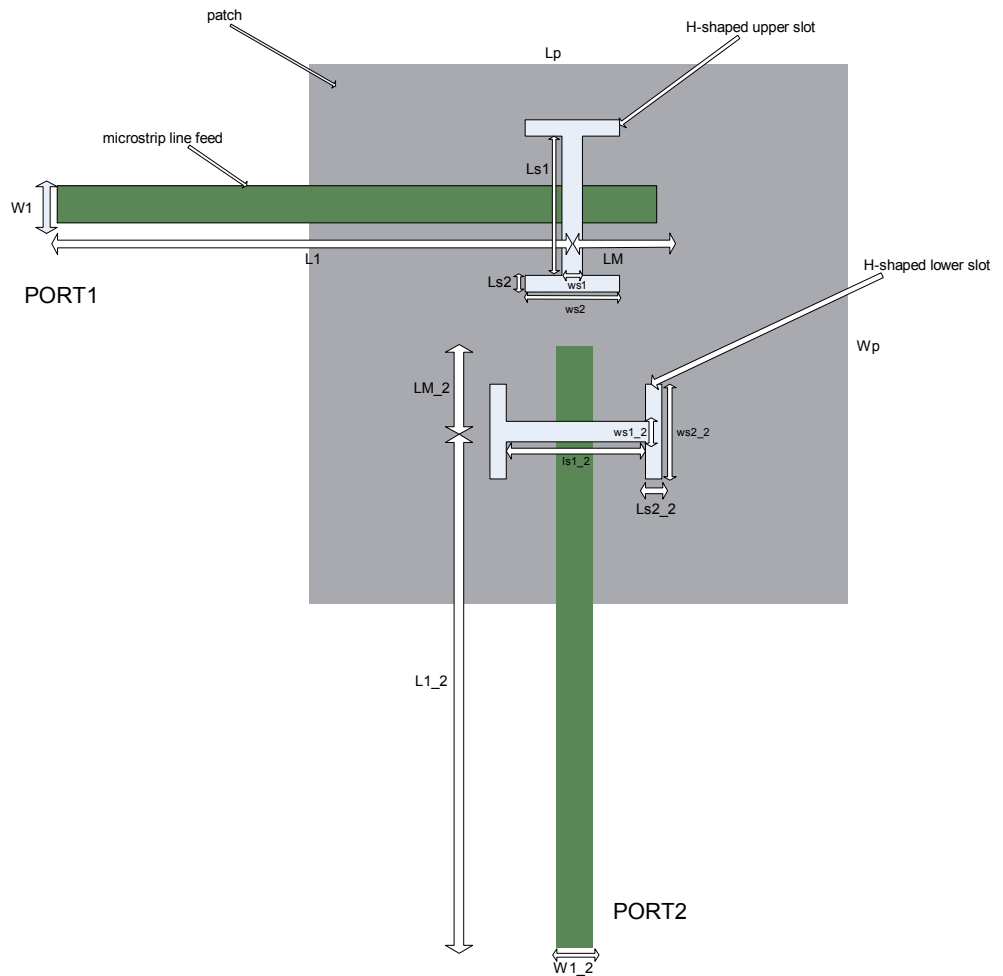


Figure 3-35 Top view of dual H-shaped slot coupled patch antenna structure

Throughout the parametric analysis experience is gained about the effects of critical design parameters on the resonance frequency, bandwidth and input impedance of H-shaped aperture coupled patch antennas.

The simulation results obtained with optimized antenna parameters for infinite size ground plane is given in Figure 4-1.

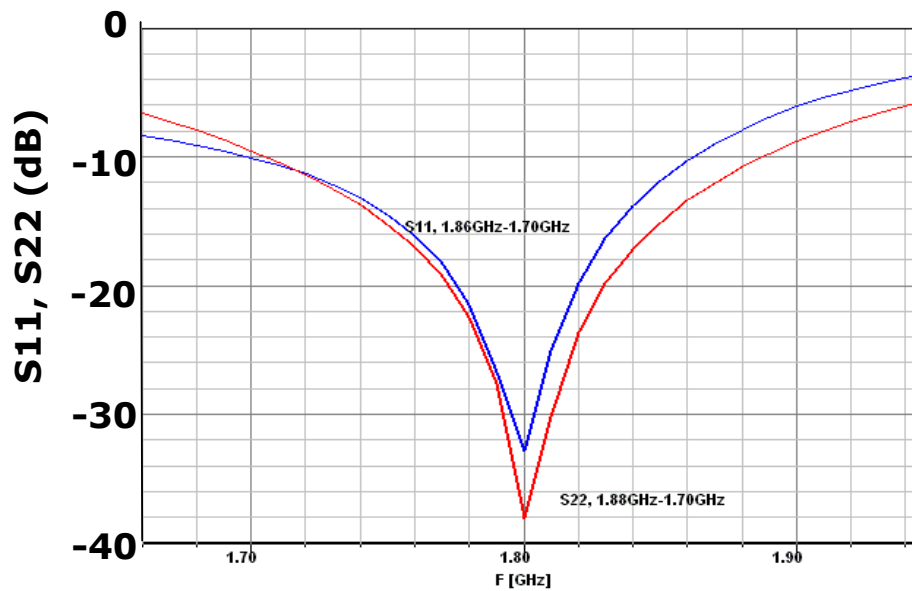


Figure 3-36 Return loss graph for S11 and S22 with an infinite ground plane.

With the help of this experience, the design parameters of the antenna are optimized and the final values are listed in Table 3-3.

Table 3-3 Optimized parameters of dual H-shaped slot coupled microstrip patch.

| Design Parameter | Value |
|-----------------------------------------------------------------|---------|
| L_p =patch length | 50mm |
| W_p =patch width | 50mm |
| xof = patch offset for the upper H slot in x direction | 0mm |
| yof = patch offset for the upper H slot in y direction | 12mm |
| xof_2= patch offset for the lower H slot in x direction | 0mm |
| yof_2= patch offset for the lower H slot in y direction | -6mm |
| ws1=width of upper H slot center leg | 0.5mm |
| ws2=width of upper H slot side leg | 22mm |
| ls1=length of upper H slot center leg | 12mm |
| ls2=length of upper H slot side leg | 1mm |
| L_1 = Microstrip feedline length for upper H-shaped slot | 50mm |
| W_1 = Microstrip feedline width for upper H-shaped slot | 1.181mm |
| L_M = Stub length for upper H-shaped slot | 7mm |
| ws1_2=width of lower H slot center leg | 0.5mm |
| ws2_2=width of lower H slot side leg | 17mm |
| ls1_2=length of lower H slot center leg | 17mm |
| ls2_2=length of lower H slot side leg | 1mm |
| L_{1_2} = Microstrip feedline length for lower H-shaped slot | 44mm |
| W_{1_2} = Microstrip feedline width for lower H-shaped slot | 1.181mm |
| L_{M_2} = Stub length for lower H-shaped slot | 7mm |

CHAPTER 4

FABRICATION AND MEASUREMENTS

The dual polarized H-shaped slot coupled microstrip patch antenna is fabricated. In scope of this chapter, fabrication will be summarized. Feed dielectric substrate and antenna dielectric substrate are ROGERS RO4003. The antenna needs to be fabricated on a finite ground plane. The size of the ground plane was taken to be 100 x 100 mm, which was an available maximum ground plane dimension for the fabrication process. To observe “the effects of finite ground plane on the radiation characteristics of the antenna”, simulations with Ansoft Designer are repeated “with a finite ground plane but with an infinite substrate”. Some deviations in the resonance frequency are observed and the parameters of the antenna are re-tuned. Figure 4-1 provides the simulation results obtained with optimized antenna parameters for finite size ground plane.

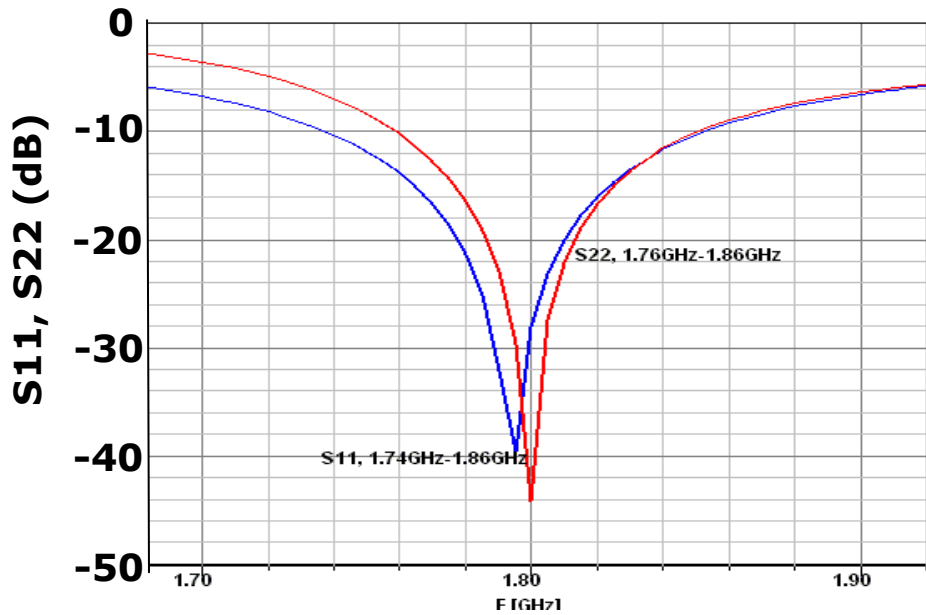
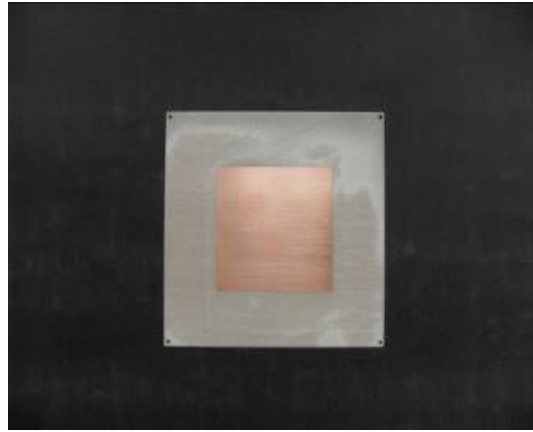


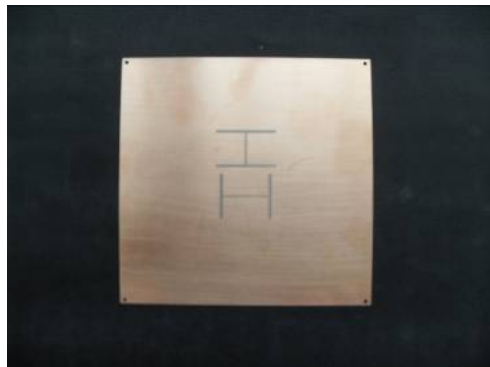
Figure 4-1 Return loss graph for S11 and S22 with a finite ground plane.

Laser PCB scraping equipment in ASELSAN is used for obtaining the patch, H-shaped slots and microstrip lines. Before scraping the paths on the PCB, the design files of the Ansoft Designer are converted into Gerber files, which are loaded to the equipment. The laser device reads the position of the relevant objects and scraps the rest of the board by burning the copper material on the PCB.

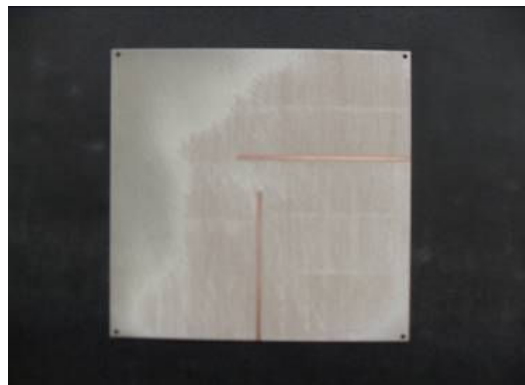
The critical part of the fabrication is attaching the foam substrate between patch layer and feed layer. “The ground plane of the feed layer is also the ground plane of the patch layer” [25]. The alignment of the patch layer, foam substrate and the feed layer was achieved with the alignment holes and screws. With the alignment holes one can match centers of apertures and patch elements as in the simulation. The screwing hole (2mm diameter) locations are selected on four edges of both the patch layer and the feed layer. Substrate material was attached between patch and feed layer by screwing through these holes. The step by step fabrication is as in Figure 4-2 and Figure 4-3:



a)



b)

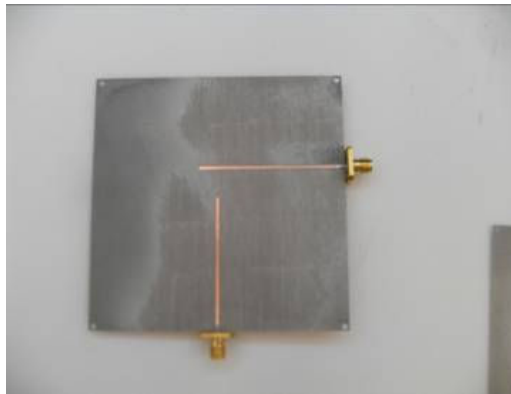


c)

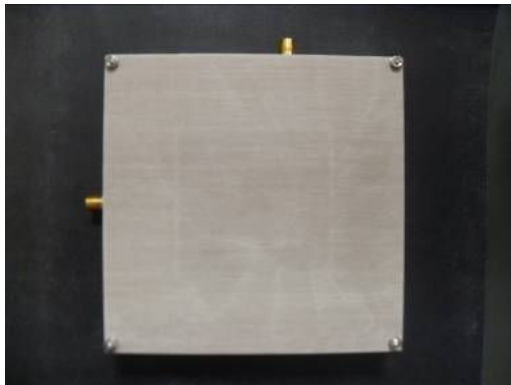
Figure 4-2 Initial fabrication process of the patch and feed layers, a) antenna patch structure, b) antenna ground plane with the H-shaped slots, c) microstrip lines feeding the patch from H-shaped slots.



a)



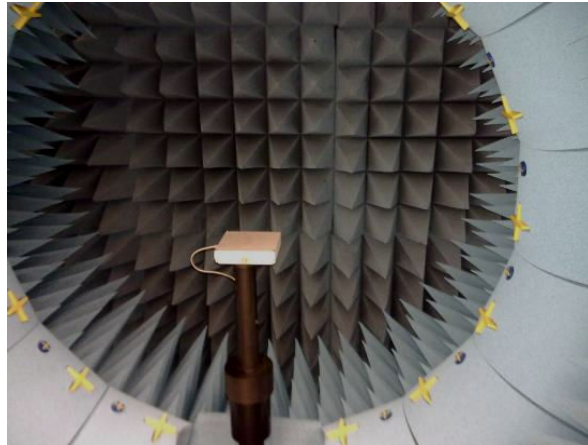
b)



c)

Figure 4-3 Fabrication process after the foam is attached between feed layer and antenna layer and connectors are mounted to the microstrip lines, a) patch on top of the foam structure, b) back view of the antenna and microstrip lines, c) top view of the antenna.

Next the fabricated antenna was tested for the S parameters by network analyzer. “Far-field radiation patterns” are obtained using the anechoic chamber facilities at ASELSAN. The set-up used for obtaining the antenna pattern is presented in Figure 4-4.



a)



b)

Figure 4-4 Antenna Radiation Pattern Measurement Set-Up, a) antenna in the anechoic chamber, b) radiation pattern measurement from port 1, so port 2 is matched with a 50ohm load.

With the aim of reducing reflections, the room walls are covered with absorbers. The prototype antenna is fixed on the set up and the feed side of the antenna was covered by an absorber to eliminate distortions on the antenna pattern caused by metallic walls.

The experimental results for the “S parameters and radiation patterns of fabricated antennas” are discussed in following sections. They are compared with the simulation results. It is found that a good agreement is achieved between them.

4.1 Results of the Antenna

Network analyzer is used to measure the S-parameters of the fabricated antenna. Figure 4-5 and Figure 4-6 provides the comparison of the experimental results and simulation results.

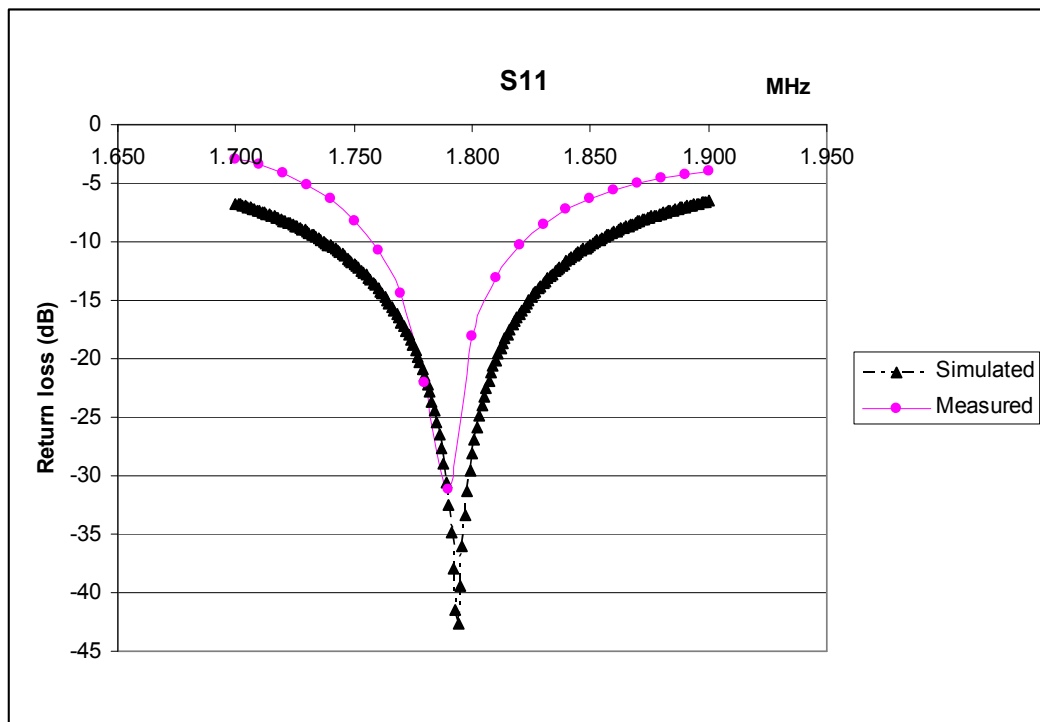


Figure 4-5 Experimental and simulation results for S11 (return loss).

Figure 4-5 shows “the return loss against frequency of the antenna for port 1 excitation and the resonant frequency” of the antenna, which occurs at 1.8GHz according to the simulation results. Within the measurement results the resonant occurs at 1.79GHz. -10dB bandwidth of the antenna obtained from measurement results is 3.5%. The bandwidth of the antenna obtained from simulation results is 6.7%.

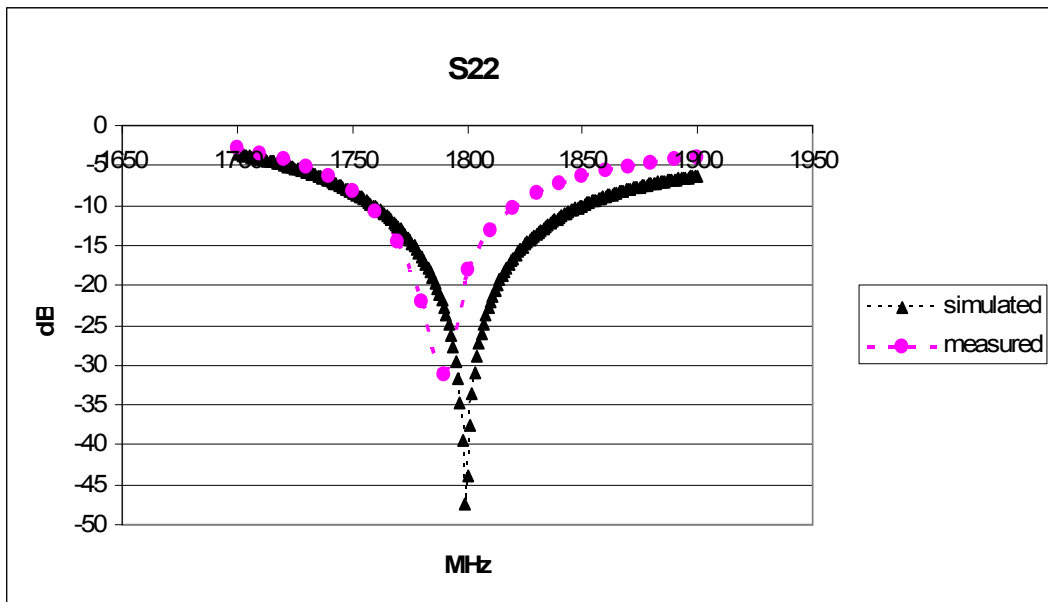


Figure 4-6 Experimental results and Simulation results for S22 (return loss).

Figure 4-6 shows “the return loss against frequency of the antenna for port 2 excitation and the resonant frequency of the antenna”, which occurs at 1.8GHz according to the simulation results. Within the measurement results the resonant occurs at 1.79GHz. -10dB bandwidth of the antenna obtained from measurement results is 4.5%. The bandwidth of the antenna obtained from simulation results is 6.5%.

For the S11 and S22 graphs the measurement results are shifted above the simulation results. The “metallic connectors at the port 1 and port 2 of the prototype antenna” may be the other reason of the difference. The existence of the connectors may cause the loss and mismatch between microstrip lines. If the measurement trace is shifted to the same level with the simulation trace, it would be observed that the bandwidth is quite similar to the simulation value of bandwidth.

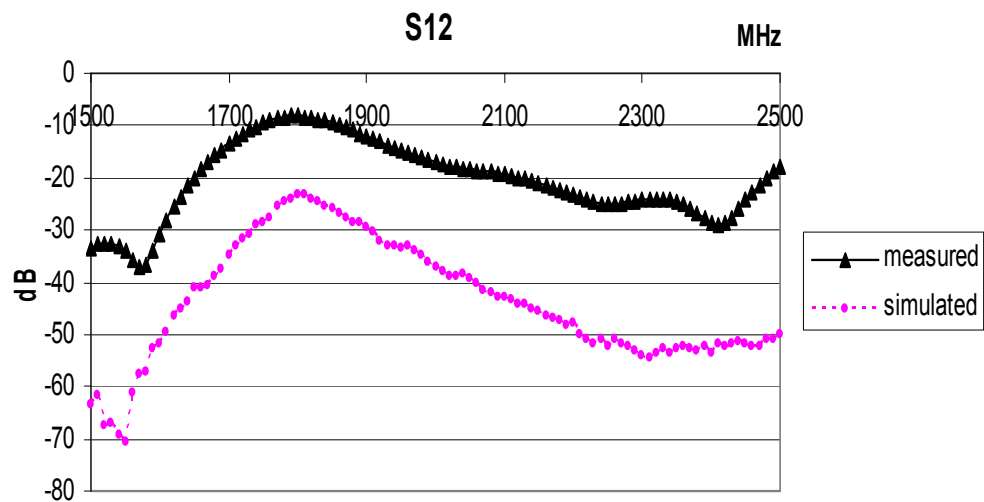


Figure 4-7 Experimental and simulation results for S12 (Isolation between port 1 and port 2).

Figure 4-7 provides “the isolation between port 1 and port 2”. From the simulation results the isolation within the frequency band of interest is smaller than -23.4 dB. From the measurement results port 1 isolation from port 2 is less than -8.3 dB.

The mismatches between the measurement and the simulation for the isolation are estimated to be related with the coupling of the ports.

Another reason of this shift may be the finite dielectric substrate above the patch or finite dielectric substrate of the feed part. Since dielectric of antenna substrate is infinite for simulation model and finite for fabrication model, this causes the reflection of surface waves in the substrate.

“Radiation patterns of the antenna for E-plane and H-plane” results are provided in “Figure 4-8, Figure 4-9, Figure 4-11 and Figure 4-10”.

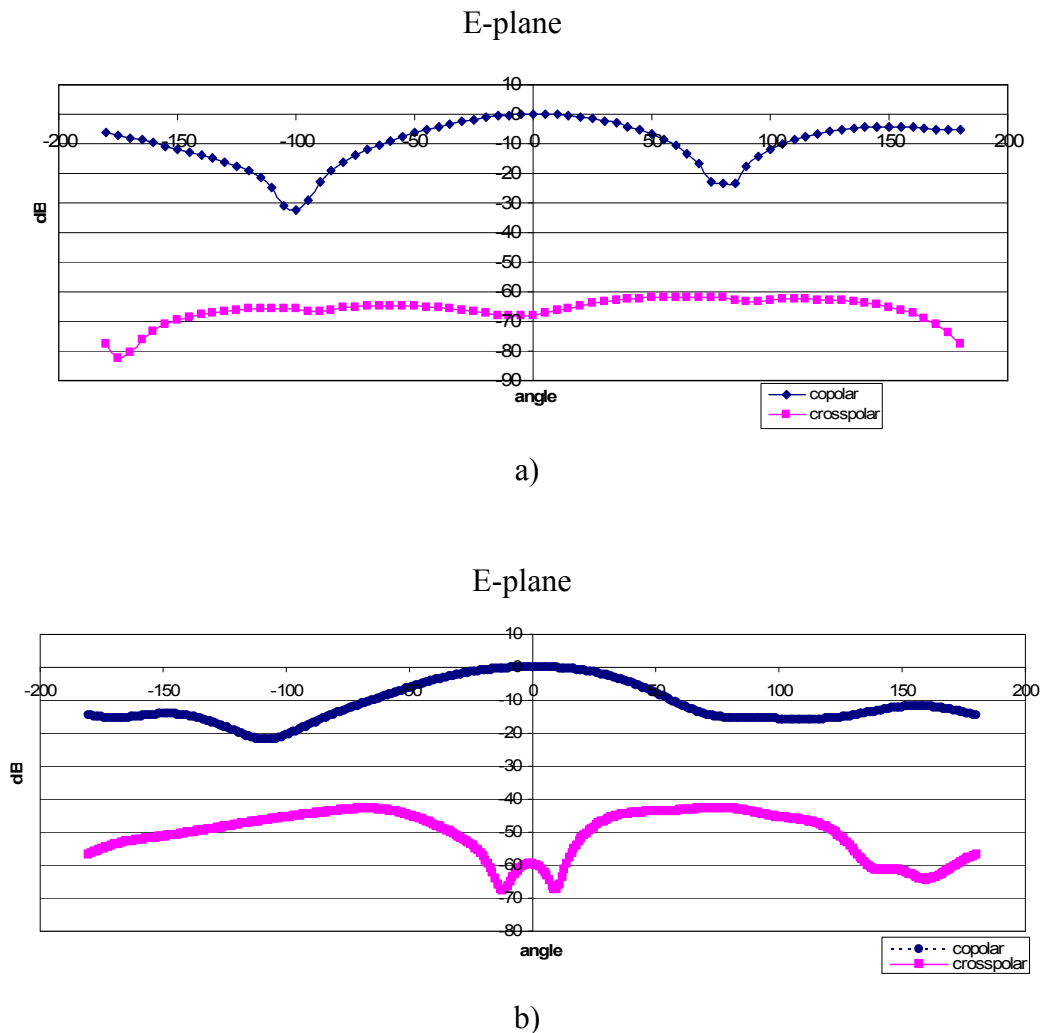
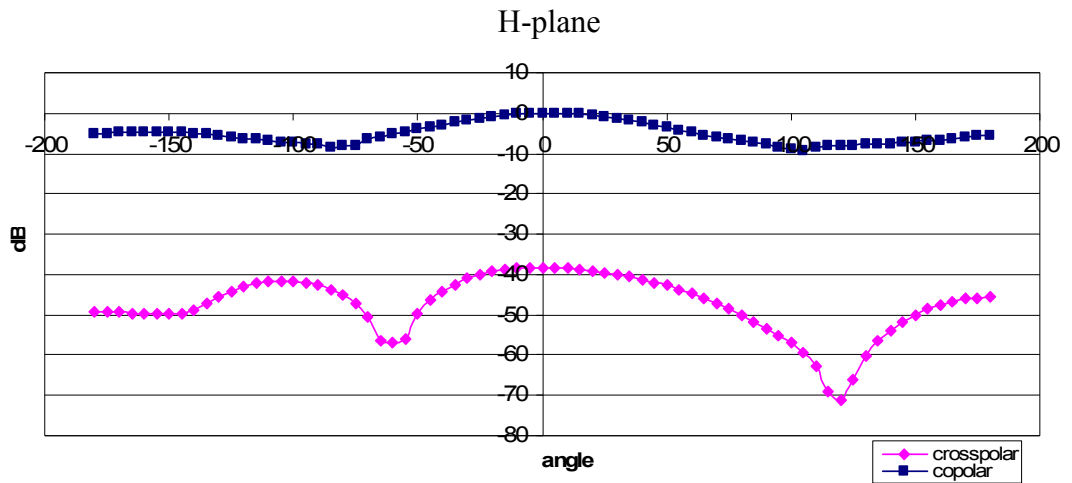
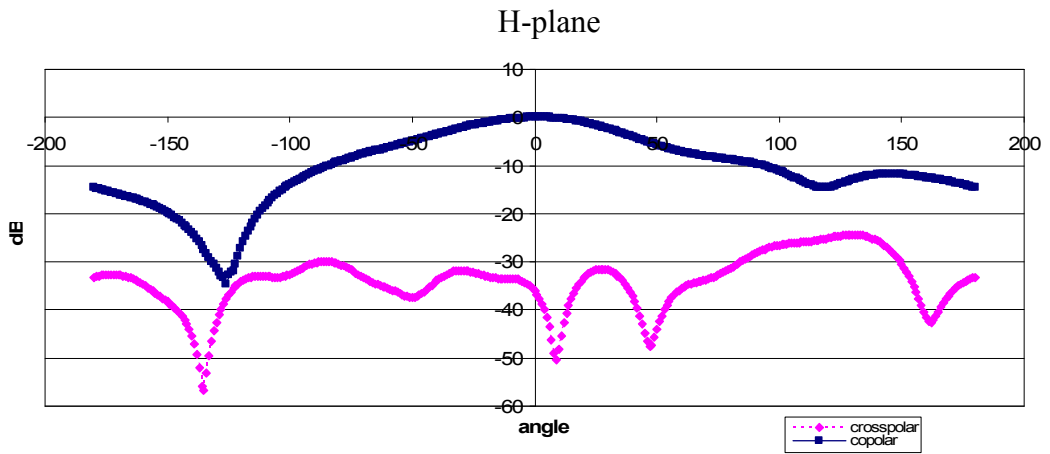


Figure 4-8 Radiation pattern characteristics port 1 excitation for a) simulation
 b) measurement results respectively, E-plane.

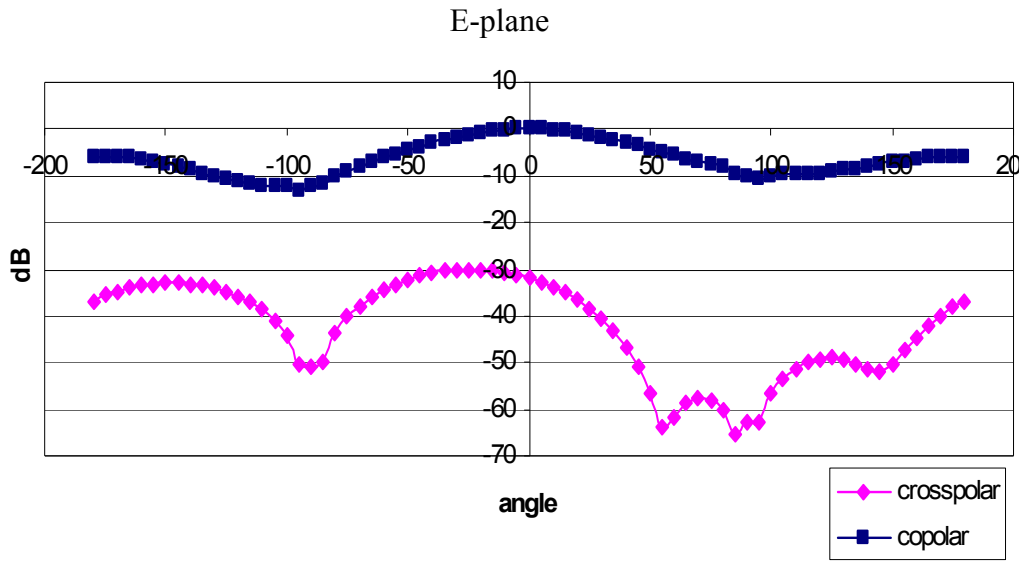


a)

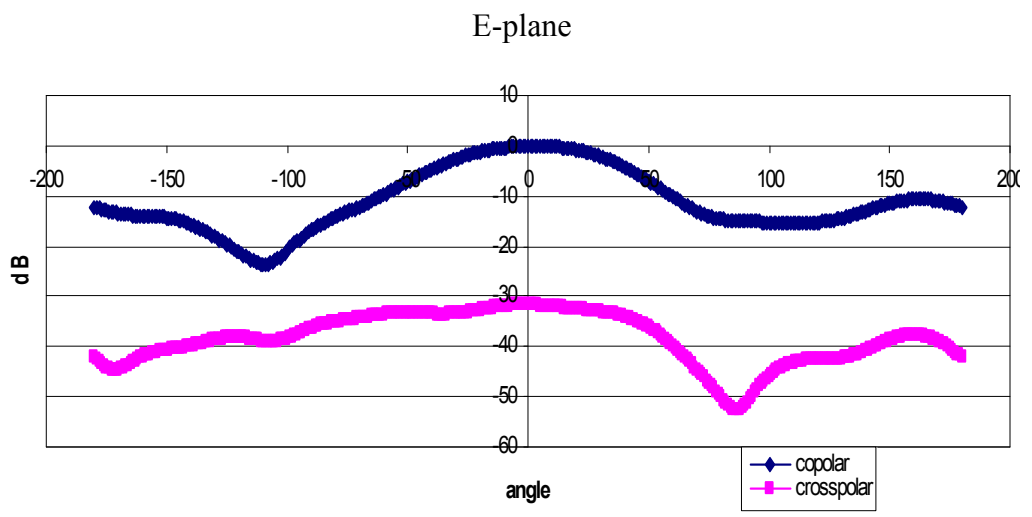


b)

Figure 4-9 Radiation pattern characteristics port 1 excitation for
 a) simulation, b) measurement results respectively, H-plane.

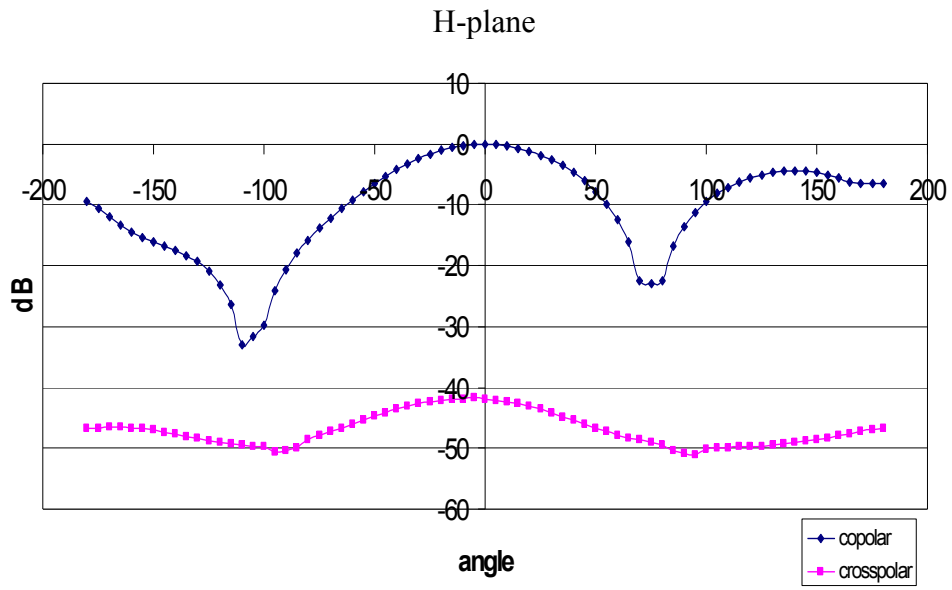


a)

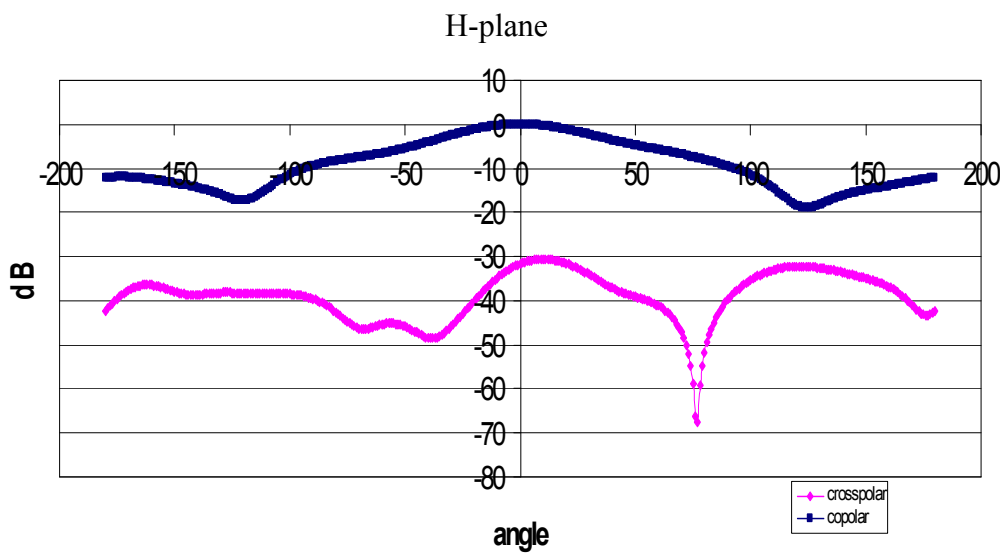


b)

Figure 4-10 Radiation pattern characteristics port 2 excitation for a) simulation
b) measurement results respectively, E-plane.



a)



b)

Figure 4-11 Radiation pattern characteristics port 2 excitation for a) simulation
b) measurement results respectively, H- plane,

From the results of simulation and measurement radiation pattern, it is observed that with a dual polarized antenna a low cross polarization level can be obtained. Cross polarization levels are for port 1 < -35 dB,, for port 2 < -30 dB for each principle planes.

CHAPTER 5

CONCLUSIONS AND FUTURE WORK

In this thesis slot coupled microstrip patch antennas and dual polarized H-shaped slot coupled patch antennas are studied. The microstrip rectangular patch antennas studied in this thesis are:

1. A rectangular microstrip patch antenna with a rectangular-shaped slot,
2. A rectangular microstrip patch antenna with an H-shaped slot,
3. A dual polarized rectangular patch antenna with two H-shaped slots.

The radiation pattern and return loss characteristics of these antennas have been studied in terms of their resonance frequencies. The parametric analysis was performed for each design to observe the effect of antenna parameters on resonance frequencies and bandwidth characteristics of the antennas. -10dB bandwidths were studied extensively for each design. The simulations were conducted with Ansoft Designer electromagnetic simulation program.

In first step, rectangular-shaped slot coupled patch antenna parametric analysis was studied and the same analysis was realized for the H-shaped slot coupled patch antenna. The same bandwidth and resonant frequency characteristics were obtained with smaller size H-shaped slot than a rectangular-shaped slot. The advantage of using a H-shaped slot rather than a rectangular-shaped slot is proven.

Dual polarized H-shaped slot coupled microstrip patch antenna was also analyzed and implemented within the scope of this thesis. The dual-polarized operation was performed by double slots, each are H-shaped and positioned on the ground plane in

“T” formation providing a good isolation level among port 1 and port 2. The parametric analysis was performed for this structure and optimized design values were obtained. For fabrication process finite ground plane was also modeled in Ansoft Designer. The analysis was also performed to obtain the optimized values with finite ground plane. Using the optimized design results a dual-polarized H-shaped slot coupled microstrip antenna is produced and measured.

Comparison between design simulations and measurements has been studied in order to investigate the critical production parameters causing deviation from the design. The reasons of the deviations from the simulation model may be connectors used within the prototype antenna.

Acceptable agreements with the simulated and experimental results are observed for resonance frequency. The shift of measurement results from the simulation results in the return loss graphs may be caused by the connectors in the prototype antenna which is not included in the simulations.

For the future work dual polarized H-shaped slot coupled microstrip patch antenna for different resonant frequencies can be developed. Besides additional bandwidth widening techniques can be applied for the implementation of alternative H-shaped slot coupled microstrip patch antennas. Number of H-shaped slots can be increased in order to obtain multiple resonant frequencies.

Other alternative as a future work is using multiple dual polarized H-shaped slot coupled microstrip patch antennas in an array structure for an electronic defense or a radar system. It is obvious that as long as the computational power and simulation tools improve, it will be possible to implement various applications of slot coupled patch antennas considering the advantages proven within this thesis.

REFERENCES

- [1] G.A. Deschamps, "Microstrip Microwave Antennas", Presented at the 3rd USAF Symposium On Antennas, 1953.
- [2] J.Q. Howell, "Microstrip Antennas", IEEE APS Int. Symp. Digest, pp. 177-180, 1972.
- [3] R.E. Munson, "Conformal Microstrip Antennas and Microstrip Phased Arrays", IEEE Trans. Antennas Propagation, Vol. AP-22, pp. 74-78, 1974.
- [4] D. M. Pozar, "Microstrip Antennas," Proc. IEEE, Vol. 80, No.1, pp. 79-81, January 1992.
- [5] C. A. Balanis, "Antenna Theory Analysis and Design Second Edition", John Wiley & Sons, United States of America, 1997.
- [6] J. F. Zurcher and F. E. Gardiol, "Broadband Patch Antennas", Artech House, United States of America, 1995.
- [7] S. D. Targonski, R. B. Waterhouse and D. M. Pozar, "Design of Wide-Band Aperture-Stacked Patch Microstrip Antennas", IEEE Transactions on Antennas and Propagation, Vol. 46, No. 9, September 1998.
- [8] K.F. Lee, K.M. Luk, K.F. Tong, S.M. Shum, T. Huynh and R.Q. Lee, "Experimental and Simulation Studies of the Coaxially fed U-Slot Rectangular Patch Antenna", IEE Proc. Microwave and Antennas Propagation, Vol. 144, No. 5, October 1997.
- [9] S.K. Palit, A. Hamadi, "Design and Development of Wideband and Dual-band Microstrip Antennas", IEE Proc. Microwave and Antennas Propagation, Vol. 146, No. 1, February 1999.

- [10] A. Lehto and A. Raisanen, RF-Ja Mikroaaltotekniikka, 7th edn. Otatieto, 2002.
- [11] R.Q. Lee, K.F. Lee and J. Bobinchak, "Characteristics of a two-layer electromagnetically coupled rectangular patch antenna", Electronics Letters, Vol. 23, pp. 1070-1072, 1987.
- [12] G. Kumar and K. P. Ray, "Broadband Microstrip Antennas", Artech House, United States of America, 2003.
- [13] A. Lamminen, "Design of Millimeter-wave Antennas on Low Temperature Co-fired Ceramic Substrates", M. Sc. Thesis, Helsinki University of Technology, Helsinki, Finland, 2006.
- [14] J. C. MacKinchan, et al., "A Wide Bandwidth Microstrip Sub-Array for Array Antenna Application Using Aperture Coupling," IEEE AP-S Int. Symp. Digest '1989' pp.878-881.
- [15] D. M. Pozar, "A Microstrip Antenna Aperture Coupled to a Microstrip Line", Electronics Letters, Vol. 21, pp. 49-50, January 17, 1985.
- [16] S. Gao, L. Li, M. Leong and T. Yeo "Dual Polarized Slot Coupled Planar Antenna with Wide Bandwidth", IEEE Trans. on Antennas and Propagation, Vol. AP-51, pp. 441-448, 2003.
- [17] V. Rathi, G. Kumar, .K.P. Ray, "Improved Coupling for Aperture Coupled Microstrip Antennas", IEEE Trans. on Antennas and Propagation, Vol. AP-44, pp. 1196-1198, 1996.
- [18] H.S. Shin, N. Kim, "Wideband and High Gain One-Patch Microstrip Antenna Coupled with H-Shaped Aperture", Electronics Letters, Vol. 38, pp. 1072-1073, 2002.

- [19] S. Gao and A. Sambell “Simple Broadband Dual-polarized Printed Antenna”, *Microwave and Optical Technology Letters*, Vol. 46, pp. 144-148, July 2005.
- [20] L. Shafai, "Chapter IV: Microstrip Antennas", 24.427 Antennas Course Notes, University of Manitoba, Canada, pp. 43-64, 1998.
- [21] J. P. Kim, “Analysis and Network Modeling of an Aperture-Coupled Microstrip Patch Antenna”, *IEEE Trans. on Antennas and Propagation*, Vol. 49, No. 6, pp. 849-854, June 2001.
- [22] P.L. Sullivan and D.H. Schaubert, “Analysis of an Aperture Coupled Antenna”, *IEEE Trans. on Antennas and Propagation*, Vol. AP-34, pp. 977-984, August 1986.
- [23] D. M. Pozar and D. H. Schaubert, “Scan blindness in infinite phased arrays of printed dipoles,” *IEEE Trans. on Antennas and Propagation*, Vol. AP-32, pp. 602-620, June 1984.
- [24] J. R. James and P. S. Hall, *Handbook of Microstrip Antennas*, Vols. 1 and 2, Peter Peregrinus, London, UK, 1989.
- [25] R. Bhalla, “Analysis of Broadband and Dual Band Microstrip Patch Antennas”, M. Sc. Thesis, University of Manitoba, Manitoba, Canada, 2001.
- [26] G. Parker, Y.M.M. Antar “A dual polarized microstrip ring antenna with good isolation”
- [27] Tzung-Wern Chiou and Kin-Lu, “Wong, A Compact Dual-Band Dual-Polarized Patch Antenna for 900/1800-MHz Cellular Systems” *IEEE transactions on Antennas and Propagation*, Vol. 51, No. 8, August 2003.
- [28] D. M. Pozar, *Microwave Engineering*, John Wiley & Sons, Inc., 2nd Edition.

APPENDIX A

Microstrip Line Parameters

Microstrip line is a planar transmission line as shown in Figure 5-1(a). For practical applications the dielectric substrate is thin ($d \ll \lambda$) so the fields are quasi TEM. The air and dielectric substrate introduce nonhomogeneous region for the electric field lines which are shown in Figure 5-1(b). The effective dielectric constant can be defined as the dielectric constant of the homogeneous medium replacing both air and dielectric substrate regions of the microstrip line. By introducing effective dielectric constant, a uniform dielectric material is obtained as in Figure 5-1(c).

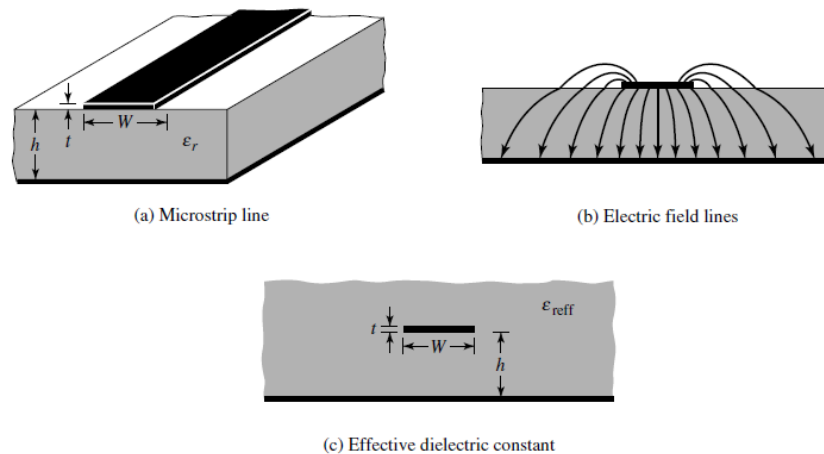


Figure 5-1 Electric field lines and effective dielectric constant geometry of microstrip patch antenna [5].

The effective dielectric constant, ϵ_{reff} , is expressed as [28]

$$\epsilon_{eff} = \frac{\epsilon_r + 1}{2} + \frac{\epsilon_r - 1}{2} \left(1 + \frac{12h}{W}\right)^{-1/2}$$

The characteristic impedance of the microstrip line is given by [28]

$$Z_0 = \frac{60}{\sqrt{\epsilon_{eff}}} \ln\left(\frac{8h}{W} + \frac{W}{4h}\right) \quad \text{for } W/h < 1$$

$$Z_0 = \frac{120\pi}{\left[\frac{W}{h} + 1.393 + 0.667 \ln\left(\frac{W}{h} + 1.444\right)\right] \sqrt{\epsilon_{eff}}} \quad \text{for } W/h > 1$$